we used four different isolates from both human and animal hosts, the strains ER52, ER53, ER54 and ER60. These strains belong to the B2 subgroup (typical of extraintestinal *E. coli*) of the *E. coli* standard collection of reference and express different amounts of α-haemolysin (Lai *et al.*, 1999). Vesicle preparations from the four strains were isolated and analysed (Fig. 8A). Immunoblot analysis using anti-α-haemolysin antisera confirmed the presence of α-haemolysin in the vesicles isolated from the four strains and haemolytic activity assays confirmed that the α-haemolysin in the OMVs was active (data not shown). Studies of the protein profile of the vesicles by detecting specific components of the outer and inner membranes indicated that the vesicles produced by these strains were in all cases OMVs (data not shown). Using the quantitative determination of OmpA by Western blot as an estimation of OMVs produced, the strains ER52, ER54 and ER60 produce apparently the same amount of

OMVs. Interestingly the strain ER53 seems to produce a significant lower amount of OMVs (sixfold lower amount of OmpA was detected). The percentage of the soluble and OMVs-associated α-haemolysin was estimated and found to vary dependent on the strain. The average percentage of OMVs-associated α-haemolysin was 2.5%, 1.7%, 14.3% and 31.4% for the strains ER52, ER53, ER54 and ER60 respectively. The values were lower than in the case of strain MC1061 (66%) mentioned above but rather similar to estimates obtained with *E. coli* K-12 derivatives W3110 and MG1655 (17% and 11% respectively).

Outer membrane vesicles produced by the strain ER60 were visualized by atomic force microscopy (Fig. 8B). Similarly to what was described above for the α-haemolysin producing K-12 strains two types of vesicles were found: small vesicles with a diameter of approximately 50–70 nm and a minor subpopulation of larger vesicles with a diameter of 150–200 nm. We conclude that the features of OMVs from the laboratory strains are found also in the cases of natural and clinical *E. coli* isolates.
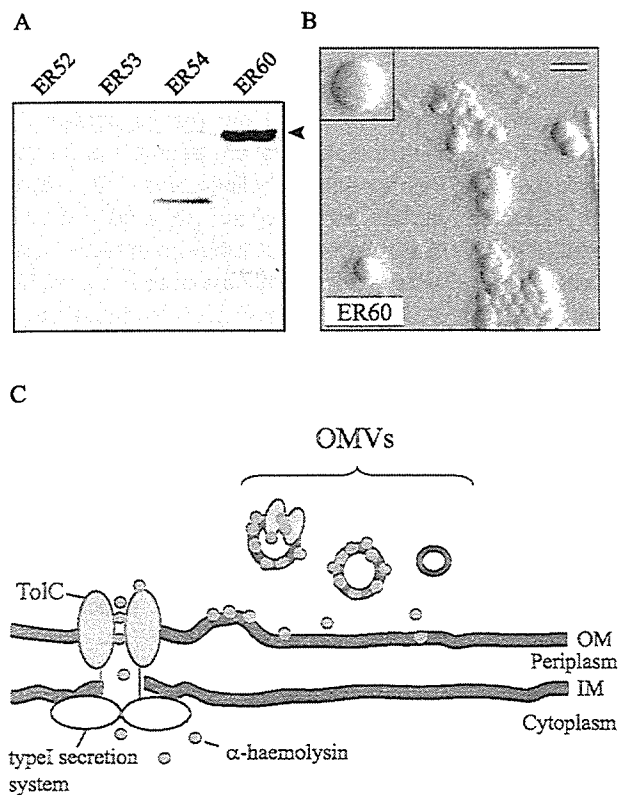
Discussion

The secretion of the α-haemolysin is the prototype for the type I secretion system, a *sec*-independent system where the proteins are translocated in a one-step process to the extracellular media in a soluble form, without a periplasmic intermediate (see model in Fig. 8C). The present study establishes that a clearly recognizable fraction of the secreted α-haemolysin is, in fact, associated with OMVs. Analyses of the vesicle fraction by dissociation assays and density gradients showed that the α-haemolysin was tightly associated with the OMVs. Interestingly, OMVs fractionation and EM structural studies suggested that the OMVs containing α-haemolysin are characterized by their larger size, thinner margin and lower density when compared with the non-α-haemolysin containing OMVs. Moreover, our results showed that the protein composition was different between the two types of OMVs and we found that a type I machinery component, the TolC protein, was associated to the α-haemolysin containing OMVs. These results suggest that the α-haemolysin is preferentially localized in OMVs with a particular protein composition. Most of the experiments performed in this work were done in the *E. coli* strain MC1061, which was empirically chosen by being a high OMVs producer strain. The strain MC1061 is *galE*15 *galU galK*16 (Casadaban and Cohen, 1980), which might affect LPS composition. However, the localization of the α-haemolysin in OMVs was also observed in wild-type strains such as W3110 and MG1655 (Fig. 5 and C. Balsalobre, unpubl. data) and the ECOR strains (Fig. 8A), ruling out the possibility that the phenotype observed was unique for a particular strain. Tests with an *rfaG* mutant derivative of strain W3110 indi-

Fig. 8. The localization of α-haemolysin in OMVs is a common feature among haemolytic *E. coli* strains.
A. Immunoblot analysis of vesicles from the strains ER52, ER53, ER54 and ER60 using anti-α-haemolysin antisera. The band corresponding to the α-haemolysin is indicated with an arrowhead. In the gel the OMVs isolated from 10 ml supernatant of a culture with an OD600 of 0.8 were loaded.
B. Atomic force microscopy imaging of OMVs from strain ER60. The insert highlights an example of the larger vesicles in the preparation. Bar equals to 100 nm.
C. Model of secretion and OMVs localization of the α-haemolysin (see text).

cated that a higher percentage of α-haemolysin was localized to the OMVs when compared with the wild-type isogenic strain (our unpublished data). Perhaps the LPS structure of the bacteria can influence the localization of the α-haemolysin. This could then be the reason for the observed differences with different natural isolates. Furthermore, that would also provide a possible explanation for the earlier reported phenotypes of rough LPS-producing strains that showed a decrease in the amount of active secreted α-haemolysin (Stanley *et al.*, 1993; Wandersman and Letoffe, 1993; Bauer and Welch, 1997).

The production of OMVs is a common phenomenon for most Gram-negative bacteria (Beveridge, 1999). The role of OMVs in export and targeting of bacterial toxins is an emerging new concept. It has been proposed that the heteromeric heat-labile enterotoxin (LT) produced by enterotoxigenic *E. coli* (ETEC), after it is secreted to the extracellular milieu by the general secretion pathway, is interacting with the LPS and released from the bacterial surface by OMVs (Horstman and Kuehn, 2002). Recently, it has been shown that an OMVs-mediated transport pathway is responsible for both (i) the export of the pore-forming cytolysin A (ClyA) from the bacteria and (ii) the activation of the ClyA cytotoxin by altering its redox status (Wai *et al.*, 2003). The mechanism of secretion of the α-haemolysin, by the periplasmic-independent type I pathway, differs completely from the toxins described above and there is no resemblance in protein sequence or structure. Our present results indicate that export of secreted proteins via OMVs not necessarily would require a periplasmic localization of the proteins during the secretion process. It seems likely that the protein transport to the extracellular milieu via OMVs may occur independently of the mechanism of protein secretion.

Our findings provide the first evidence that physiologically active α-haemolysin is associated with OMVs. However, the HlyC-mediated acylation, which is essential for the activity, was evidently not required for the localization of the α-haemolysin in the OMVs (Fig. 5). Previous studies have shown that the acylation of the α-haemolysin is not required for the stable association of the α-haemolysin with erythrocytes (Bauer and Welch, 1996; Moayeri and Welch, 1997). An intriguing question is whether the localization of the α-haemolysin in OMVs affects the activity of the toxin compared with the soluble form. At present, it is not possible for us to provide answer to this but we conclude that both forms were active. The well documented instability of the α-haemolysin (Welch, 1991) and the experimental design of the process of purification of OMVs did not allow us to quantitatively compare the activities of the two forms of the toxin.

A schematic model is summarized in Fig. 8C. An intriguing possibility is that formation of OMVs occasionally may occur where the type I secretion machinery is assembled. As a consequence, the α-haemolysin protein, perhaps together with some secretion system components (e.g. TolC), would be incorporated into the OMVs before leaving the bacterial cell. If so, the secretion system may affect the composition of the OMVs. At present we have no detailed information about the localization, topology and possible functional interactions of the proteins in the OMVs. Future studies will hopefully reveal if, e.g. TolC and/or other components are forming a type I secretion pore structure or if they may generate a special type of OMVs when localized with the Hly proteins. It will also be of interest to assess if accessory proteins like HlyB and/or HlyD are appearing in the OMVs.

All the results described here are compatible with the current model of how the α-haemolysin is translocated over the bacterial envelope when secreted by the type I secretion system from *E. coli*. Our findings are also consistent with the earlier reported observation that secreted α-haemolysin appeared to be localized on the surface of the bacteria (Oropeza-Wekerle *et al.*, 1989). After secretion to the extracellular space the α-haemolysin presumably binds to the bacterial surface and then it may be released in a relatively concentrated fashion by being associated with the OMVs. All our results obtained by different approaches (dissociation assays, proteinase susceptibility, immunogold labelling and the inability of externally added α-haemolysin to bind MC1061/pACYC184 OMVs) suggest that the α-haemolysin associated to the OMVs is not entirely exposed but somehow protected by the OMV structure (Fig. 2). No proteinase K digestion was detected when the vesicle structure was intact (no detergent added). Interestingly, an intense deposition of gold particles was only detected in areas where vesicles structures seemed disrupted. When intact vesicles were observed, little or no gold deposition was detected (Fig. 2E). These results are consistent with the suggestion that the α-haemolysin in the intact vesicles is not exposed and was only recognized by the monoclonal antibody when disruption of the vesicle structure had occurred.

Our results obtained by both biochemical and microscopy methods suggested a localization of the α-haemolysin not much exposed on the surface of the OMVs when we studied native samples of (i.e. non-fixed) OMVs. In the work by Oropeza-Wekerle *et al.* (1989), the α-haemolysin was detected in association with the cell-membranes by using immunogold labelling with polyclonal anti-α-haemolysin antisera on glutaraldehyde-fixed cells. Methodological differences between these studies may explain the apparent differential degree of exposure of the toxin when associated with membranes.

Another type I secreted protein has been described to be associated to membrane vesicles, the leukotoxin of *Actinobacillus actinomycetemcomitans*. Characterization

of the membrane vesicles produced by this bacterium showed that the membrane vesicles are enriched in active leukotoxin (Kato *et al.*, 2002; Demuth *et al.*, 2003). This would suggest that the protein association to outer membrane vesicles might be a common process among the type I secreted proteins.

The association of the α-haemolysin with the OMVs may play an important role in the pathogenicity of extraintestinal α-haemolysin-producing *E. coli* isolates, such as UPEC. The results obtained using the natural and clinical isolates confirmed that the dissemination of the α-haemolysin by OMVs is a common feature among haemolytic *E. coli* strains. *In vivo* experiments have shown the relevant role of the α-haemolysin in the pathogenicity of UPEC (Welch *et al.*, 1981; Hacker *et al.*, 1983). Moreover, *in vitro* studies indicated that the α-haemolysin has cytotoxic and/or cytolytic effects against a wide variety of cell types, including erythrocytes, neutrophils, granulocytes, epithelial cells, etc. (Lally *et al.*, 1999). Based on the present findings we suggest that OMVs may play a role in the dissemination of the α-haemolysin to the host cells and targets during extraintestinal *E. coli* infections. It will be of interest to assess their properties further and to determine the role of the OMVs carrying α-haemolysin in the pathogenicity of *E. coli* in different types of infections. The molecular events involved in delivery of the α-haemolysin from the OMVs to the eukaryotic cell is unknown at the moment. Studies on the transport of the heat-labile enterotoxin by OMVs have shown that the ETEC vesicles are internalized by an endocytic process (Kesty *et al.*, 2004). Presumably, the α-haemolysin present in OMVs could be delivered in a similar manner and further studies will hopefully clarify this question. These findings should also prompt investigations regarding the potential of other type I secreted proteins to localize to OMVs and how components of the type I secretion machinery may influence the formation and/or properties of OMVs.

Experimental procedures

Bacterial strains and plasmids

The *E. coli* strains used in this work were: MC1061 (Casadaban and Cohen, 1980), W3110 (Jensen, 1993), MG1655 (Jensen, 1993), Hb2151(Carter *et al.*, 1985), J96 (Hull *et al.*, 1982) and the isolates ER52, ER53, ER54 and ER60 (Ochman and Selander, 1984). The plasmids used were: pACYC184 (Chang and Cohen, 1978), the plasmid pANN202-312R (Godessart *et al.*, 1988) that carries the whole *hlyCABD* operon cloned in pACYC184, the plasmid pBR322 (Bolivar *et al.*, 1977), the plasmids pANN202-812 and pANN202-812B (Ludwig *et al.*, 1987) that carry the whole *hlyCABD* operon cloned in pBR322, pANN202-812B that carries a *hlyC* mutant by a frameshift in aa position 141 of HlyC, the plasmid pEHlyA (Tzschaschel *et al.*, 1996)

and the plasmid pVDL9.3 (Fernandez and de Lorenzo, 2001).

Isolation of bacterial vesicles

The vesicles were isolated from bacterial cultures grown aerobically at 37°C to late log-phase in LB broth essentially as described earlier (Wai *et al.*, 1995; 2003). The isolation of OMVs was performed at late log-phase, when the expression of the α-haemolysin reaches the maximum level, as shown earlier (Mourino *et al.*, 1994). That our bacterial strains showed the same expression pattern was confirmed by determination of the amount of OMVs material and α-haemolysin through the growth curve by determination of the protein profile. Furthermore, the analysis showed that OMVs were released during all growth phases as well (data not shown). Bacterial cells were removed by centrifugation (6 000 *g*, 15 min, 4°C) and sequentially the supernatants were filtered through a 0.45 μm-pore-size vacuum filter. Vesicles were collected by ultracentrifugation (150 000 *g*, 180 min, 4°C) in a 45 Ti rotor (Beckman Instrument). The supernatants were carefully removed and the vesicles were suspended in 20 mM Tris HCl (pH 8.0), unless otherwise indicated. The absence of bacterial cells from vesicle preparations was routinely confirmed by viable count tests on L plates. Vesicles preparations were kept at −20°C.

SDS-PAGE and Western immunoblotting analyses

The standard SDS-PAGE procedure was used (Laemmli, 1970). Gels were stained with Coomassie blue or silver stain. For immunoblotting, we used the methods described earlier (Towbin *et al.*, 1979). Different antibodies were used as the primary antibodies: polyclonal anti-α-haemolysin (Balsalobre *et al.*, 1996), polyclonal anti-TolC (Thanabalu *et al.*, 1998), polyclonal anti-OmpA (Henning *et al.*, 1979) and polyclonal anti-CRP (Johansson *et al.*, 2000) sera; and monoclonal anti-α-haemolysin antibody E2 (Pellett *et al.*, 1990) and monoclonal anti-E tag antibody (Amersham Biosciences). For detection we used a horseradish peroxidase-conjugate antibody and the ECL⁺ chemiluminiscence system (Amersham Biosciences).

Dissociation assays

Vesicles in 50 mM HEPES were incubated for 60 min on ice in absence or presence of either NaCl (1 M), Na_2CO_3 (0.1 M), Urea (0.8 M) or Triton X-100 (0.5%). After incubation samples were centrifuged (20 800 *g*, 180 min, 4°C). Both soluble (supernatant) and particulate (pellet) fractions were analysed by SDS-PAGE. Prior to loading, the soluble proteins present in the supernatants were concentrated by trichloroacetic acid precipitation.

Proteinase K susceptibility assay

The proteinase K susceptibility assay was carried out as previously described (Cheng and Schneewind, 2000). Briefly, vesicles were treated at 37°C for 30 min in 20 mM Tris HCl

(pH 8.0) with proteinase K (0.5 µg ml⁻¹) in either absence or presence of 1% SDS. In parallel control experiments, 1 mM PMSF was added to inhibit the proteinase K activity. Following the incubation, all samples were placed on ice and 1 mM PMSF was added to quench all proteolysis, and the samples were analysed by SDS-PAGE.

Attachment of free α-haemolysin to OMVs

The ability of free α-haemolysin to attach to OMVs was assayed using active α-haemolysin purified by elution from SDS-polyacrylamide gel in PBS. SDS was removed by dialysis against PBS. The calcium-dependent haemolytic activity was determined as described below. A total of 5 µg of purified α-haemolysin was mixed in 50 mM HEPES with OMVs isolated from 20 ml culture supernatant from strain MC1061/pACYC184. After 30 min on ice samples were centrifuged (20 800 g, 180 min, 4°C). Both soluble (supernatant) and particulate (pellet) fractions were analysed by SDS-PAGE. Prior to loading, the soluble proteins present in the supernatants were concentrated by trichloroacetic acid precipitation. Control with no addition of OMVs was performed.

Cell fractionation

Cell fractions containing either the outer or the inner membranes were obtained from late log-phase cultures of MC1061/pANN202-312R in LB medium. Cells were harvested (6 000 g, 15 min, 4°C) and washed in HE Buffer (10 mM HEPES pH 7.8, 0.5 mM EDTA). Cells were disrupted by 1 min sonication (10 s pulses, 30% amplitude) and unbroken cells were removed by centrifugation (9 000 g, 5 min, 4°C). The outer and inner membrane fractions were obtained as described previously (Horstman and Kuehn, 2000).

NADH oxidase activity assay

The NADH oxidase activity of 30 µg total protein of either the vesicles or the inner and outer membrane fractions was measured as previously described (Horstman and Kuehn, 2000). The protein concentration was measured using the BCA Protein Assay Reagent Kit (Pierce).

Assay of haemolytic activity

Quantitative haemolytic assay was performed essentially as described previously (Oscarsson *et al.*, 1999). Briefly, a 20% horse blood suspension was prepared in either 0.9% NaCl or 0.9% NaCl containing 10 mM CaCl₂. In 96-well microtitre plates 50 µl of blood suspension was mixed with an equal amount of different dilutions of the vesicles and incubated for 60 min at 37°C. Thereafter, 100 µl of ice-cold 0.9% NaCl was added and the microtitre plate was centrifuged (400 g, 15 min, 4°C). The haemolytic activity was monitored as the release of haemoglobin, measured spectrophotometrically at 540 nm. The amount of vesicles in samples from strains MC1061/pACYC184 and MC1061/pANN202-312R used in the haemolytic assay was standardized by the amount of OmpA protein.

Assay for HeLa cell detachment

Cell detachment was assayed on semiconfluent monolayer of HeLa cells cultured in MEM Eagle (Sigma) with 10% fetal calf serum in 24-well tissue culture plates. HeLa cells monolayers were washed three times with PBS-CM (phosphate-buffered saline with 0.01% CaCl₂ and 0.01% MgCl₂), and 1 ml of PBS-CM was added to each well. In total, 10 µl sample (bacterial culture, culture supernatant, vesicles suspension or buffer) was added and the plate was incubated at 37°C for 90 min under 5% CO₂. Cell monolayers were washed three times with PBS-CM, fixed with 70% methanol for 10 min, stained with 0.13% crystal violet for 10 min, and then briefly destained in water. Cell detachment was quantified by eluting crystal violet with a solution of 50% ethanol and 1% SDS, and measuring the absorbance of the eluate at 590 nm. The amount of the vesicles added from MC1061/pANN202-312R was adjusted such that it contained the same amount of α-haemolysin present in 10 µl of bacterial culture. The amount of α-haemolysin present in bacterial culture and in culture supernatant after filtration was the same as estimated by SDS-PAGE (data not shown). The amount of vesicles added from control strain was adjusted by comparing the amount of OmpA in the vesicles of both MC1061/pANN202-312R and MC1061/pACYC184 strains.

Outer membrane vesicles fractionation

Assay performed as described (Horstman and Kuehn, 2000). Briefly, the OMVs were isolated as described above but suspended in 50 mM HEPES (pH 6.8), adjusted to 45% Optiprep (SIGMA) in 0.15 ml and transferred to the bottom of a 12 ml ultracentrifugation tube. Different Optiprep/HEPES layers were sequentially added as follows: 0.9 ml 35%, 0.9 ml 30%, 0.66 ml 25%, 0.66 ml 20%, 0.33 ml 15% and 0.33 ml 10%. Gradients were centrifuged (180 000 g, 180 min, 4°C). Fractions of equal volumes were sequentially removed and analysed by SDS-PAGE.

Electron microscopy

Ultrastructural analysis of vesicles was performed by negative staining technique as before (Wai *et al.*, 1995) using 0.5% uranyl acetate and examined by a JEM2000ET electron microscope (JEOL, Akishima, Tokyo, Japan) at 100 KV. Immunogold localization using monoclonal anti-α-haemolysin antibody E2 (Pellett *et al.*, 1990) was performed using 10 nm diameter gold particles as previously described (Wai *et al.*, 1998).

Atomic force microscopy

Outer membrane vesicles preparations were diluted with ultrapure water (Millipore) and immediately placed on a freshly cleaved mica surface. The samples were incubated at room temperature for 5 min, gently washed with ultrapure water and dried in a desiccator for at least 2 h. Imaging was performed on a Nanoscope IIIa Atomic Force Microscope (Digital Instruments) using Tapping Mode. The pictures are presented in amplitude mode.

Analysis of pulse-labelled proteins

Cultures of the strain MC1061/pANN202-312R in rich MOPS without methionine (37°C, OD_{600} of 0.7) were labelled by addition of 60 μCi [^{35}S]Methionine per millilitre (6 × 10^{-8} M). Incorporation of isotope was terminated at 20 s by addition of non-radioactive methionine (8 × 10^{-3} M). At different time points (0, 30, 60 and 300 s) after addition of non-radioactive methionine 1 ml samples were taken and soluble and vesicles fractions were separated as described above (20 800 *g*, 180 min, 4°C). The samples were analysed by SDS-PAGE.

Thin-layer chromatography

The studies on the phospholipid content were performed by TLC using Silica gel 60 plates and developing in chloroform-methanol-water (75:25:2.5, by volume). After allowing sufficient time for drying, the phospholipids were detected by spraying the plate with ethanolic phosphomolybdic acid reagent (10%), followed by charring in an oven.

Acknowledgements

References

Balsalobre, C., Juarez, A., Madrid, C., Mourino, M., Prenafeta, A., and Munoa, F.J. (1996) Complementation of the *hha* mutation in *Escherichia coli* by the *ymoA* gene from *Yersinia enterocolitica*: dependence on the gene dosage. *Microbiology* **142** (Part 7): 1841–1846.

Bauer, M.E., and Welch, R.A. (1996) Association of RTX toxins with erythrocytes. *Infect Immun* **64**: 4665–4672.

Bauer, M.E., and Welch, R.A. (1997) Pleiotropic effects of a mutation in *rfaC* on *Escherichia coli* hemolysin. *Infect Immun* **65**: 2218–2224.

Beveridge, T.J. (1999) Structures of Gram-negative cell walls and their derived membrane vesicles. *J Bacteriol* **181**: 4725–4733.

Bolivar, F., Rodriguez, R.L., Greene, P.J., Betlach, M.C., Heyneker, H.L., and Boyer, H.W. (1977) Construction and characterization of new cloning vehicles. II. A multipurpose cloning system. *Gene* **2**: 95–113.

Carter, P., Bedouelle, H., and Winter, G. (1985) Improved oligonucleotide site-directed mutagenesis using M13 vectors. *Nucleic Acids Res* **13**: 4431–4443.

Casadaban, M.J., and Cohen, S.N. (1980) Analysis of gene control signals by DNA fusion and cloning in *Escherichia coli*. *J Mol Biol* **138**: 179–207.

Chang, A.C., and Cohen, S.N. (1978) Construction and characterization of amplifiable multicopy DNA cloning vehicles derived from the P15A cryptic miniplasmid. *J Bacteriol* **134**: 1141–1156.

Cheng, L.W., and Schneewind, O. (2000) *Yersinia enterocolitica* TyeA, an intracellular regulator of the type III machinery, is required for specific targeting of YopE, YopH, YopM, and YopN into the cytosol of eukaryotic cells. *J Bacteriol* **182**: 3183–3190.

Demuth, D.R., James, D., Kowashi, Y., and Kato, S. (2003) Interaction of *Actinobacillus actinomycetemcomitans* outer membrane vesicles with HL60 cells does not require leukotoxin. *Cell Microbiol* **5**: 111–121.

Felmlee, T., and Welch, R.A. (1988) Alterations of amino acid repeats in the *Escherichia coli* hemolysin affect cytolytic activity and secretion. *Proc Natl Acad Sci USA* **85**: 5269–5273.

Fernandez, L.A., and de Lorenzo, V. (2001) Formation of disulphide bonds during secretion of proteins through the periplasmic-independent type I pathway. *Mol Microbiol* **40**: 332–346.

Fernandez, L.A., Sola, I., Enjuanes, L., and de Lorenzo, V. (2000) Specific secretion of active single-chain Fv antibodies into the supernatants of *Escherichia coli* cultures by use of the hemolysin system. *Appl Environ Microbiol* **66**: 5024–5029.

Godessart, N., Munoa, F.J., Regue, M., and Juarez, A. (1988) Chromosomal mutations that increase the production of a plasmid-encoded haemolysin in *Escherichia coli*. *J Gen Microbiol* **134**: 2779–2787.

Hacker, J., Hughes, C., Hof, H., and Goebel, W. (1983) Cloned hemolysin genes from *Escherichia coli* that cause urinary tract infection determine different levels of toxicity in mice. *Infect Immun* **42**: 57–63.

Henning, U., Schwarz, H., and Chen, R. (1979) Radioimmunological screening method for specific membrane proteins. *Anal Biochem* **97**: 153–157.

Horstman, A.L., and Kuehn, M.J. (2000) Enterotoxigenic *Escherichia coli* secretes active heat-labile enterotoxin via outer membrane vesicles. *J Biol Chem* **275**: 12489–12496.

Horstman, A.L., and Kuehn, M.J. (2002) Bacterial surface association of heat-labile enterotoxin through lipopolysaccharide after secretion via the general secretory pathway. *J Biol Chem* **277**: 32538–32545.

Hull, S.I., Hull, R.A., Minshew, B.H., and Falkow, S. (1982) Genetics of hemolysin of *Escherichia coli*. *J Bacteriol* **151**: 1006–1012.

Jensen, K.F. (1993) The *Escherichia coli* K-12 'wild types' W3110 and MG1655 have an *rph* frameshift mutation that leads to pyrimidine starvation due to low *pyrE* expression levels. *J Bacteriol* **175**: 3401–3407.

Johansson, J., Balsalobre, C., Wang, S.Y., Urbonaviciene, J., Jin, D.J., Sonden, B., and Uhlin, B.E. (2000) Nucleoid proteins stimulate stringently controlled bacterial promoters: a link between the cAMP-CRP and the (p)ppGpp regulons in *Escherichia coli*. *Cell* **102**: 475–485.

Kadurugamuwa, J.L., and Beveridge, T.J. (1995) Virulence factors are released from *Pseudomonas aeruginosa* in association with membrane vesicles during normal growth and exposure to gentamicin: a novel mechanism of enzyme secretion. *J Bacteriol* **177**: 3998–4008.

Kato, S., Kowashi, Y., and Demuth, D.R. (2002) Outer membrane-like vesicles secreted by *Actinobacillus actino-*

mycetemcomitans are enriched in leukotoxin. *Microb Pathog* **32**: 1–13.

Kesty, N.C., Mason, K.M., Reedy, M., Miller, S.E., and Kuehn, M.J. (2004) Enterotoxigenic *Escherichia coli* vesicles target toxin delivery into mammalian cells. *EMBO J* **23**: 4538–4549.

Kolling, G.L., and Matthews, K.R. (1999) Export of virulence genes and Shiga toxin by membrane vesicles of *Escherichia coli* O157:H7. *Appl Environ Microbiol* **65**: 1843–1848.

Koronakis, V. (2003) TolC – the bacterial exit duct for proteins and drugs. *FEBS Lett* **555**: 66–71.

Laemmli, U.K. (1970) Cleavage of structural proteins during the assembly of the head of bacteriophage T4. *Nature* **227**: 680–685.

Lai, X.H., Wang, S.Y., and Uhlin, B.E. (1999) Expression of cytotoxicity by potential pathogens in the standard *Escherichia coli* collection of reference (ECOR) strains. *Microbiology* **145**: 3295–3303.

Lally, E.T., Hill, R.B., Kieba, I.R., and Korostoff, J. (1999) The interaction between RTX toxins and target cells. *Trends Microbiol* **7**: 356–361.

Ludwig, A., Vogel, M., and Goebel, W. (1987) Mutations affecting activity and transport of haemolysin in *Escherichia coli*. *Mol Gen Genet* **206**: 238–245.

Moayeri, M., and Welch, R.A. (1997) Prelytic and lytic conformations of erythrocyte-associated *Escherichia coli* hemolysin. *Infect Immun* **65**: 2233–2239.

Mourino, M., Munoa, F., Balsalobre, C., Diaz, P., Madrid, C., and Juarez, A. (1994) Environmental regulation of alpha-haemolysin expression in *Escherichia coli*. *Microb Pathog* **16**: 249–259.

Nicaud, J.M., Mackman, N., Gray, L., and Holland, I.B. (1986) The C-terminal, 23 kDa peptide of *E. coli* haemolysin 2001 contains all the information necessary for its secretion by the haemolysin (Hly) export machinery. *FEBS Lett* **204**: 331–335.

Ochman, H., and Selander, R.K. (1984) Standard reference strains of *Escherichia coli* from natural populations. *J Bacteriol* **157**: 690–693.

Oropeza-Wekerle, R.L., Muller, E., Kern, P., Meyermann, R., and Goebel, W. (1989) Synthesis, inactivation, and localization of extracellular and intracellular *Escherichia coli* hemolysins. *J Bacteriol* **171**: 2783–2788.

Oscarsson, J., Mizunoe, Y., Li, L., Lai, X.H., Wieslander, A., and Uhlin, B.E. (1999) Molecular analysis of the cytolytic protein ClyA (SheA) from *Escherichia coli*. *Mol Microbiol* **32**: 1226–1238.

Pellett, S., Boehm, D.F., Snyder, I.S., Rowe, G., and Welch, R.A. (1990) Characterization of monoclonal antibodies against the *Escherichia coli* hemolysin. *Infect Immun* **58**: 822–827.

Saunders, N.B., Shoemaker, D.R., Brandt, B.L., Moran, E.E., Larsen, T., and Zollinger, W.D. (1999) Immunogenicity of intranasally administered meningococcal native outer membrane vesicles in mice. *Infect Immun* **67**: 113–119.

Shoberg, R.J., and Thomas, D.D. (1993) Specific adherence of *Borrelia burgdorferi* extracellular vesicles to human endothelial cells in culture. *Infect Immun* **61**: 3892–3900.

Stanley, P.L., Diaz, P., Bailey, M.J., Gygi, D., Juarez, A., and Hughes, C. (1993) Loss of activity in the secreted form of *Escherichia coli* haemolysin caused by an *rfaP* lesion in

core lipopolysaccharide assembly. *Mol Microbiol* **10**: 781–787.

Stanley, P., Koronakis, V., and Hughes, C. (1998) Acylation of *Escherichia coli* hemolysin: a unique protein lipidation mechanism underlying toxin function. *Microbiol Mol Biol Rev* **62**: 309–333.

Thanabalu, T., Koronakis, E., Hughes, C., and Koronakis, V. (1998) Substrate-induced assembly of a contiguous channel for protein export from *E. coli*: reversible bridging of an inner-membrane translocase to an outer membrane exit pore. *EMBO J* **17**: 6487–6496.

Towbin, H., Staehelin, T., and Gordon, J. (1979) Electrophoretic transfer of proteins from polyacrylamide gels to nitrocellulose sheets: procedure and some applications. *Proc Natl Acad Sci USA* **76**: 4350–4354.

Tzschaschel, B.D., Guzman, C.A., Timmis, K.N., and de Lorenzo, V. (1996) An *Escherichia coli* hemolysin transport system-based vector for the export of polypeptides: export of Shiga-like toxin IleB subunit by *Salmonella typhimurium aroA*. *Nat Biotechnol* **14**: 765–769.

Wai, S.N., Takade, A., and Amako, K. (1995) The release of outer membrane vesicles from the strains of enterotoxigenic *Escherichia coli*. *Microbiol Immunol* **39**: 451–456.

Wai, S.N., Mizunoe, Y., Takade, A., Kawabata, S.I., and Yoshida, S.I. (1998) *Vibrio cholerae* O1 strain TSI-4 produces exopolysaccharide materials that determine colony morphology, stress resistance, and biofilm formation. *Appl Environ Microbiol* **64**: 3648–3655.

Wai, S.N., Lindmark, B., Soderblom, T., Takade, A., Westermark, M., Oscarsson, J., *et al*. (2003) Vesicle-mediated export and assembly of pore-forming oligomers of the enterobacterial ClyA cytotoxin. *Cell* **115**: 25–35.

Wandersman, C., and Delepelaire, P. (1990) TolC, an *Escherichia coli* outer membrane protein required for hemolysin secretion. *Proc Natl Acad Sci USA* **87**: 4776–4780.

Wandersman, C., and Letoffe, S. (1993) Involvement of lipopolysaccharide in the secretion of *Escherichia coli* alpha-haemolysin and *Erwinia chrysanthemi* proteases. *Mol Microbiol* **7**: 141–150.

Welch, R.A. (1991) Pore-forming cytolysins of Gram-negative bacteria. *Mol Microbiol* **5**: 521–528.

Welch, R.A., Dellinger, E.P., Minshew, B., and Falkow, S. (1981) Haemolysin contributes to virulence of extraintestinal *E. coli* infections. *Nature* **294**: 665–667.

Supplementary material

The following supplementary material is available for this article online:

Fig. S1. The association of HlyA with the vesicles is highly resistant to urea. Dissociation assays using vesicles from MC1061/pANN202-312R and increasing concentration of urea. Samples of vesicles in 20 mM Tris-HCl pH 8.0 with 0, 1.5 and 8 M of urea were incubated for 60 min on ice. The samples were then centrifuged and the resulting pellets (P) and supernatants (S) were analysed by 10% SDS-PAGE and silver stained. The protein band corresponding to the haemolysin is indicted with an arrowhead.

Fig. S2. The carboxi terminal domain of HlyA is not sufficient for the localization of HlyA in the OMVs. Expression of the carboxi terminal domain of HlyA from plasmid pEHlyA was

induced in different genetic backgrounds by addition of IPTG (0.25 mM; 90 min) and immunoblot analyses using anti-Etag and anti-OmpA antisera were performed. Lanes 1–4, samples from cultures of the strain Hb2151 carrying the plasmids pVDL9.3 (hlyB and hlyD) and pEHlyA (E-tagged C-HlyA); lanes 5–7, samples from cultures of the strain MC1061 carrying the plasmids pANN202-312R and pEHlyA. Lane 1: total extract before IPTG addition; lane 2 and 5: total extract after IPTG induction; lanes 3 and 6: soluble proteins precipitated from supernatant obtained after induction of EHlyA expression; lanes 4 and 7: OMVs isolated after induction of EHlyA expression.

Fig. S3. Analyses of phospholipid composition by thin-layer chromatography (TLC).

A. Total extract (lanes 1 and 2) and OMVs (lanes 3 and 4) of MC1061/pACYC184 (lanes 1 and 3) and MC1061/pANN202-312R (lanes 2 and 4); lane C: phosphatydilethanolamine.

B. Lanes 1 and 2 as in A. Lane 3: Optiprep fraction No. 9 (big OMVs, containing α-haemolysin). Lane 4: Optiprep fraction No. 15 (small OMVs).

This material is available as part of the online article from http://www.blackwell-synergy.com

Increased biofilm formation in *Escherichia coli* isolated from acute prostatitis

Sojun Kanamaru [a], Hisao Kurazono [b], Akito Terai [c], Koichi Monden [d], Hiromi Kumon [d], Yoshimitsu Mizunoe [e], Osamu Ogawa [a], Shingo Yamamoto [f,*]

[a] *Department of Urology, Graduate School of Medicine, Kyoto University, Kyoto, Japan*
[b] *Department of Veterinary Public Health, Graduate School of Life and Environmental Sciences, Osaka Prefecture University, Sakai, Japan*
[c] *Department of Urology, Kurashiki Central Hospital, Kurashiki, Japan*
[d] *Department of Urology, Okayama University Graduate School of Medicine and Dentistry, Okayama, Japan*
[e] *Department of Bacteriology, Faculty of Medical Sciences, Kyushu University, Fukuoka, Japan*
[f] *Department of Urology, Hyogo College of Medicine, Hyogo, Japan*

Abstract

Using crystal violet binding assay, we examined the potential for biofilm formation in 194, 76 and 107 isolates from urine of patients with uncomplicated acute cystitis, pyelonephritis and prostatitis, respectively. The prostatitis isolates showed significantly higher optical density (OD) values compared with cystitis and pyelonephritis isolates (OD_{540}: 0.82, 0.29 and 0.43, respectively, $P < 0.0001$). Similarly, strains of serotypes O4 and O22, which were commonly isolated from prostatitis, exhibited significantly higher OD values than did other strains. Furthermore, when the 21 prostatitis isolates were examined for expression of curli fimbriae, eight of 12 strains with a high OD value, but only three of nine with a low OD value, expressed curli fimbriae ($P = 0.0195$). These results suggest an association between acute bacterial prostatitis and biofilm formation.
© 2006 Elsevier B.V. and the International Society of Chemotherapy. All rights reserved.

Keywords: Biofilm; Prostatitis; Urinary tract infection (UTI); Uropathogenic *Escherichia coli* (UPEC); *Escherichia coli*

1. Introduction

Many bacteria are able to form biofilms, which are defined as matrix-enclosed microbial populations adherent to each other and to surfaces or interfaces [1]. The formation of biofilms on surfaces can be regarded as a universal bacterial strategy for survival and for optimum positioning to effectively use available nutrients. The gel-like state, predominantly consisting of polysaccharides, prevents the access of antibacterial agents, such as antibodies, white blood cells and antibiotics, so that sessile bacterial cells in the biofilms can withstand host immune responses and are much less susceptible to antibiotics than in their non-attached individual planktonic state [2,3]. A number of chronic bacterial infections, including chronic prostatitis, are thought to be associated with biofilm infections, which are not easily erad-

icated by conventional antibiotic therapy [4–7]. However, with regard to the pathogenesis of acute urinary tract infections (UTIs), the role of biofilms has not previously been evaluated.

Escherichia coli is the most common cause of UTIs and its structures involved in biofilm formation, such as type I pili [8], S fimbrial adhesin [9] and curli [10], have been well characterized. Most of these uropathogenic *E. coli* (UPEC) strains have been shown to possess certain virulent factors (VFs) such as adhesins, iron uptake systems, synthesis of cytotoxins, and specific O:K:H serotypes, as described over the past two decades [11,12]. In addition, pathogenicity islands (PAIs), which are present on the genomes of pathogenic strains and are one of the mechanisms for horizontal VF gene transfers between the same or related species, have been reported [13,14].

Previously, we determined the prevalence of VFs including type 1 pili (*pil*), P-fimbriae (*pap*), S-/F1C-fimbriae (*sfa/foc*), afimbrial adhesin (*afaI*), aerobactin (*aer* (*iucD*)),

* Corresponding author. Tel.: +81 798 45 6366; fax: +81 798 45 6368.
E-mail address: shingoy@hyo-med.ac.jp (S. Yamamoto).

hemolysin (*hly*) and cytotoxic necrotizing factor 1 (*cnf1*), and putative VFs including catecholate siderophore receptor (*iroN*), iron-regulated gene A homologue adhesin (*iha*), group II capsule (*kpsMT*), outer membrane protease T (*ompT*) and uropathogenic specific protein (*usp*), and showed not only that *iroN, iha, kpsMT, ompT* and *usp* are most commonly found among all UPEC strains but also that *iroN* and *usp* are most commonly associated with prostatitis. These results suggested that prostatitis requires different bacterial properties and has different pathogenicity from cystitis and pyelonephritis [15].

The present study was conducted to explore the comparative biofilm formation in acute UTI isolates from different sources, and to analyse the correlations between this ability and common UPEC serogroups.

2. Materials and methods

2.1. Bacterial isolates

A total of 377 *E. coli* strains consisting of 194, 76 and 107 isolates from the urine of patients with acute cystitis, pyelonephritis and prostatitis, respectively, were obtained from our laboratory collections [16,17]. The patients had no clinical history of severe complications, such as urolithiasis, vesicoureteral reflux, neurogenic bladder, diabetes mellitus or malignant neoplasms. The diagnosis of acute UTI was based on typical clinical symptoms such as acute onset, micturition pain, local tenderness, with or without fever of cystitis, pyelonephritis or prostatitis, and more than 10^3 colony-forming units of *E. coli* per mL of the urine sample. Midstream urine samples were obtained from male patients, whereas those from female patients were obtained using a catheter.

2.2. Confocal laser scanning microscopy (CLSM) of biofilms

Sterilized glass slides (Asahi Techno Glass Corporation, Tokyo, Japan) were put into 10-mL sterile tubes and bacterial culture of *E. coli* strains was incubated at 26 °C for 48 h. After the incubation, biofilms that developed on the glass slides were stained by Live/Dead *Bac*Light Bacterial Viability Kit (Molecular Probes Inc., Eugene, OR, USA) according to the manufacturer's instructions. Biofilm architecture of representative strains was monitored by CLSM as described previously [18].

2.3. Crystal violet (CV) binding assays

Cultures were grown in colonization factor antigen broth as described elsewhere [19] and diluted in the same pre-warmed medium to give an optical density (OD) of 0.2 at 540 nm. Ten-fold dilutions of the adjusted cultures were created in the same media by adding 20 μL volumes to 180 μL

of the same pre-warmed medium and placed in each of three wells in a polystyrene 96-well microtitre plate (Corning Inc., Corning, NY, USA). All microtitre plates were incubated statically at 26 °C for 48 h. The method for determining the extent of bacterial adherence to the microtitre well surfaces has been described elsewhere [20,21]. Briefly, the bacterial supernatants were discarded after the incubation, and loosely adherent bacteria were removed by three washes with phosphate-buffered saline (pH 7.2). The microtitre plates were then inverted and allowed to dry before each well was filled with 200 μL of 1% (w/v) CV solution (Nacalai Tesque Inc., Kyoto, Japan) and incubated at room temperature for 30 min. Unbound CV was removed by three washes with water and the plates were inverted to dry. Cell-bound CV was released from the bacterial cells by the addition of 200 μL of 95% ethanol and, after incubation at room temperature for 30 min on a rotary shaker, the concentration of CV in each solution was determined by the OD reading at 540 nm.

2.4. Electron microscopy for detecting curli fimbriae expression

For negative staining, *E. coli* cells, harvested from the biofilm on the PU sheet (Olympus Optical Co. Ltd., Tokyo, Japan) after a 24-h incubation, were mixed with distilled water and the suspension was allowed to settle for 2 min on a grid. After washing with distilled water, the specimen was negatively stained with 2% uranyl formate and air dried before transmission electron microscopy (H-7000E; Hitachi, Tokyo, Japan) [18].

2.5. Statistical analysis

Comparisons of the OD values of UTIs and common UPEC serogroups were tested using Kruskal–Wallis and Scheffe tests. For the distribution of common UPEC serogroups in UTIs, the χ^2 test was used. Comparisons of OD values among UTIs in each of the common UPEC serogroups were tested using Mann–Whitney or Kruskal–Wallis tests. A value of $P < 0.05$ was considered significant. All statistical analyses were performed using the software StatView 5.0 (SAS Institute Inc., Cary, NC, USA).

3. Results

3.1. Association between OD values and biofilm architecture

To confirm that high OD_{540} values by CV binding assay represent the ability to form biofilm, several *E. coli* strains showing different OD_{540} values were subjected to CLSM. The amount of attached bacteria monitored by CLSM showed positive correlation with OD_{540} values by CV binding assay (Fig. 1).

OD$_{540}$ CLSM image
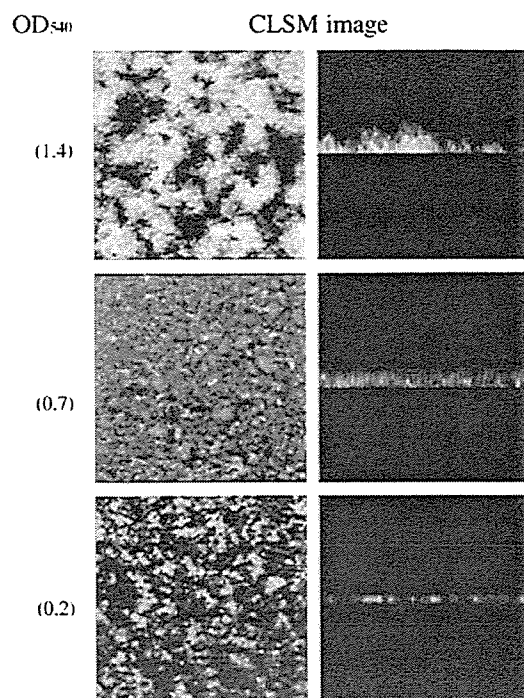

(1.4)

(0.7)

(0.2)

Fig. 1. Biofilm architectures in a static system at 26 °C for 48 h were monitored with CLSM. The OD$_{540}$ values were measured by CV binding assays under the same conditions. Horizontal and vertical sections are shown on the left and right sides, respectively. Magnification, ×200. Green, live bacteria; red, dead bacteria. CLSM, confocal laser scanning microscopy; CV, crystal violet; OD$_{540}$, optical density at 540 nm.

3.2. Adherence of UTI isolates assessed by CV binding assays

Using CV binding assays, the ability to form biofilm was determined in isolates from acute cystitis, pyelonephritis and prostatitis. Among these three categories of acute UTI, prostatitis isolates showed significantly higher OD$_{540}$ values than did cystitis and pyelonephritis isolates (median OD$_{540}$: 0.82, 0.29 and 0.43, respectively, $P < 0.0001$) (Fig. 2).

3.3. Biofilm formation in common UPEC serogroups

Among the 377 UTI isolates investigated in this study, 293 strains belonged to O1, O2, O4, O6, O16, O18, O22, O25 and O75, which are commonly found in acute UTI. As shown in
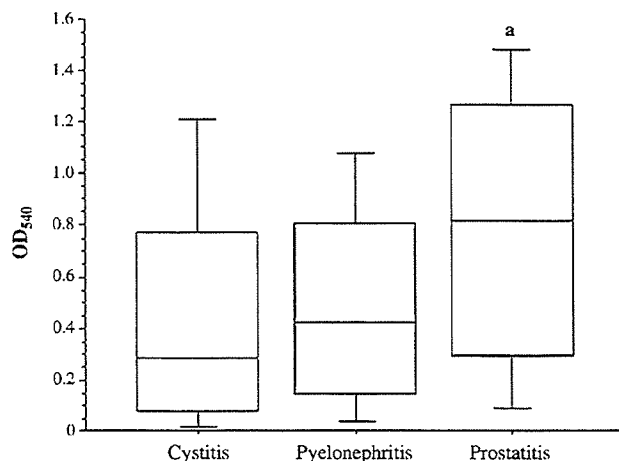

Fig. 2. Box-and-whisker plots showing the extent of biofilm formation in E. coli strains of cystitis isolates (194 strains), pyelonephritis isolates (76 strains) and prostatitis isolates (107 strains). (a) Significantly higher biofilm formation than in the cystitis and pyelonephritis isolates ($P < 0.0001$).

Table 1, strains O4 and O22 commonly caused prostatitis, whereas serogroups O1, O16, O18, O25 and O75 were commonly found in cystitis, but not in prostatitis. Interestingly, strains of these serogroups such as O4 and O22 exhibited significantly higher OD values in CV binding assays than did O1, O16, O18 and O75, suggesting that biofilm formation may contribute to causing prostatitis rather than cystitis or pyelonephritis (Fig. 3). Further, when the OD values were compared according to their source among each serogroup, isolates from prostatitis showed a higher ability to form biofilm than those from other diseases in O2, O4, O18 and O22 ($P < 0.05$, in O2 and O22, Table 2).

3.4. Correlation between biofilm formation and curli fimbriae expression

We further examined the expression of curli fimbriae in 21 prostatitis isolates with transmission electron microscopy images of negative staining. Ten of 12 strains (83%) with high OD$_{540}$ values (1.200, range 0.945–1.498) expressed curli fimbriae whereas three of nine strains with low OD$_{540}$ values (0.217, range 0.054–0.440) expressed curli fimbriae ($P = 0.0294$), indicating that curli expression is closely associated with high biofilm formation in prostatitis isolates.

Table 1
Distribution of UTI isolates in common UPEC serogroups

Origin	Isolates, N (%)								
	O1	O2	O4	O6	O16	O18	O22	O25	O75
Cystitis	22 (59.5)	22 (47.8)	7 (38.9)	12 (34.3)	22 (68.8)	36 (60.0)	4 (20.0)	8 (53.3)	19 (63.3)
Pyelonephritis	11 (29.7)	7 (15.2)	1 (5.6)	11 (31.4)	7 (21.9)	9 (15.0)	2 (10.0)	2 (13.3)	6 (20.0)
Prostatitis	4 (10.8)	17 (37.0)	10 (55.6)	12 (34.3)	3 (9.4)	15 (25.0)	14 (70.0)	5 (33.3)	5 (16.7)
Total	37	46	18	35	32	60	20	15	30

UPEC, uropathogenic E. coli; UTI, urinary tract infection.

Table 2
OD_{540} values of UTI isolates in common UPEC serogroups

O serotype	Cystitis median (interquartile range)	Pyelonephritis median (interquartile range)	Prostatitis median (interquartile range)	P-value
O1	0.21 (0.10–0.62)	0.55 (0.07–0.96)	0.28 (0.07–0.80)	0.887
O2	0.14 (0.06–0.68)	0.78 (0.51–0.83)	0.94 (0.21–1.23)	0.016[a]
O4	0.68 (0.16–1.41)	0.56	1.75 (0.87–1.67)	0.107
O6	0.36 (0.04–1.24)	0.58 (0.46–1.22)	0.16 (0.08–1.00)	0.387
O16	0.34 (0.16–0.51)	0.15 (0.08–0.22)	0.23 (0.16–0.26)	0.134
O18	0.30 (0.22–0.76)	0.32 (0.23–0.61)	0.58 (0.37–1.30)	0.229
O22	0.58 (0.23–0.99)	0.79	1.32 (0.82–1.48)	0.044[a]
O25	0.67 (0.37–1.08)	0.35	0.70 (0.61–0.83)	0.826
O75	0.10 (0.03–0.58)	0.22 (0.06–0.45)	0.24 (0.02–0.56)	0.778

O1, O2, O6, O16, O18, and O75 were analysed by the Kruskal–Wallis test.
O4, O22, and O25 were analysed by the Mann–Whitney U-test (cystitis vs. prostatitis) because the number of pyelonephritis isolates was small ($N = 1$, 2 and 2, respectively). OD_{540}, optical density at 540 nm; UPEC, uropathogenic E. coli.
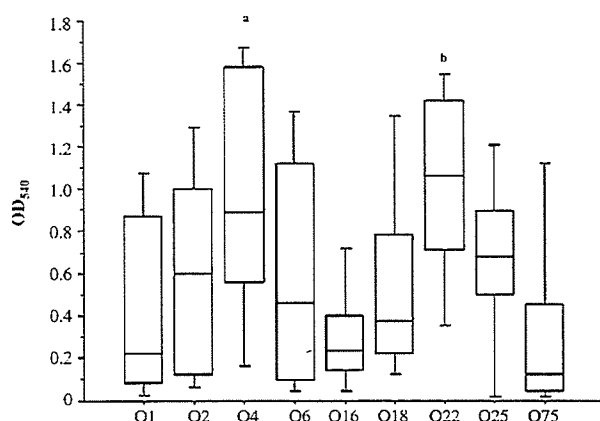[a] $P < 0.05$.

Fig. 3. Box-and-whisker plots showing the extent of biofilm formation in E. coli strains of common UPEC serogroups. UPEC, uropathogenic E. coli. (a) Significantly higher biofilm formation than for O1, O16 and O75 ($P < 0.05$). (b) Significantly higher biofilm formation than for O1, O16, O18 and O75 ($P < 0.05$).

4. Discussion

In the natural environment, bacteria are often found as sessile communities known as biofilms [1,2]. The first step in the sequence of events leading to the formation of mature biofilms is the attachment of individual cells in the aqueous phase to an available solid surface. In the case of E. coli, flagella-mediated motility is required to overcome the physical forces that repel bacteria from many types of biomaterials. On reaching the surface, pili mediate stable attachment of the cells to the device. Cell multiplication and motility then result in migration of the cells over the surface, and finally differentiation of microcolonies into mature exopolysaccharide-enclosed biofilms [4,8]. Generally, although acute UTIs can be treated effectively with antibiotics (except for cases of infection by an antibiotic-resistant strain) and are not considered to involve biofilms [4], treatments for acute prostatitis and pyelonephritis both require the use of more antibiotics than do treatment for cystitis [22,23]. In the prostate gland, in particular, once the acute infection has settled down, ther-

apy with one of the oral antimicrobial agents appropriate for the treatment of chronic bacterial prostatitis (e.g. trimethoprim or fluoroquinolones) [23] should be continued, given that many investigators have reported evidence that chronic bacterial prostatitis is due to a biofilm infection [5–7].

In this study, to determine the ability to form biofilm in acute UTI isolates (e.g. cystitis, pyelonephritis and prostatitis), CV binding assays were conducted, which represent a rapid screening method for bacterial adhesion abilities in 96-well microtitre plates [19–21]. The results showed a higher OD value, indicating a significantly higher potential of biofilm formation, in prostatitis isolates than in cystitis and pyelonephritis isolates, suggesting a close association between acute bacterial prostatitis and bacterial biofilm formation. In addition, the observation that E. coli strains of certain serogroups possessing a higher potential of biofilm formation, such as O4 and O22, predominated in prostatitis isolates would strongly support this hypothesis.

Recently, Cookson et al. reported that specific clones in Shiga-toxin-producing E. coli (O128:H2) expressing curli fimbriae could enhance biofilm formation, whereas non-expressing strains (O157:H7) failed to form biofilms [19]. In this study, we examined the expression of curli fimbriae in acute UTI isolates with transmission electron microscopy images of negative staining of representative strains, demonstrating that UPEC stains of high OD value by CV binding assay expressed curli fimbriae more frequently. The findings suggest that the ability to form biofilm among UPEC is closely correlated with the expression of curli fimbriae.

Several urovirulence factors have been known to play significant roles in the pathogenesis of bacterial prostatitis. For instance, P-fimbriae bind to urothelial receptors, and this subsequently facilitates ascent into the urinary tract as well as establishing deep infections in the prostate grand itself [22]. Furthermore, PAI-related genes (sfa/foc, hly, cnf1 and iroN) have been reported to be closely associated with prostatitis [15,17]. In this study, our data showed close associations between a higher potential of biofilm formation and some urovirulence genes, such as pil and PAI-related genes, whereas O75-related genes such as afaI, aer (iucD) and iha

[15] were associated with a lower potential of biofilm formation. Using the *E. coli* strains examined in the present study, when the correlations between biofilm formation and urovirulence factors were analysed, a higher OD value was associated with *pil*, *sfa/foc*, *hly*, *cnf1* and *iroN*, whereas a lower OD value was associated with *afaI*, *aer* (*iucD*) and *iha* (*P* < 0.05, data not shown). These results indicate that certain specific virulence genes such as *pil* and *sfa/foc* may also have significant roles in biofilm formation, consistent with previous reports [8,9].

We are also concentrating on examination of *E. coli* strains isolated from chronic prostatitis for virulence factors and biofilm formation. To date, we have completed an investigation of eight stains from chronic prostatitis, showing high OD values (0.380–0.651), as determined by CV binding assay and common presence of urovirulence factors (*sfa* 50%, *iron* 50%, *cnf1* 50%, *hly* 50%, *usp* 87.5%, *ompT* 88.9% and *iha* 25%). These results reveal that the strains isolated from chronic prostatitis show similar characteristics to those of acute prostatitis.

In summary, prostatitis strains possess many VFs and a higher potential of biofilm formation. A high potential of biofilm formation seems to be closely associated with the expression of curli fimbriae. To understand the pathogenesis in both acute and chronic prostatitis, further analyses would be required with regard to the potential of biofilm formation and the properties of VFs in UPEC causing prostatitis at different infectious phases.

References

[1] Costerton JW, Lewandowski Z, Caldwell DE, Korber DR, Lappin-Scott HM. Microbial biofilms. Annu Rev Microbiol 1995;49:711–45.

[2] Costerton JW, Cheng KJ, Geesey GG, et al. Bacterial biofilms in nature and disease. Annu Rev Microbiol 1987;41:435–64.

[3] Nickel JC, Ruseska I, Wright JB, Costerton JW. Tobramycin resistance of *Pseudomonas aeruginosa* cells growing as a biofilm on urinary catheter material. Antimicrob Agents Chemother 1985;27:619–24.

[4] Costerton JW, Stewart PS, Greenberg EP. Bacterial biofilms: a common cause of persistent infections. Science 1999;284:1318–22.

[5] Nickel JC, Costerton JW. Coagulase-negative staphylococcus in chronic prostatitis. J Urol 1992;147:398–401.

[6] Choong S, Whitfield H. Biofilms and their role in infections in urology. BJU Int 2000;86:935–41.

[7] Arakawa S, Matsui T, Gohji K, Okada S, Kamidono S. Prostatitis—the Japanese viewpoint. Int J Antimicrob Agents 1999;11:201–3.

[8] Pratt LA, Kolter R. Genetic analysis of *Escherichia coli* biofilm formation: roles of flagella, motility, chemotaxis and type I pili. Mol Microbiol 1998;30:285–93.

[9] Schmoll T, Ott M, Oudega B, Hacker J. Use of a wild-type gene fusion to determine the influence of environmental conditions on expression of the S fimbrial adhesin in an *Escherichia coli* pathogen. J Bacteriol 1990;172:5103–11.

[10] Vidal O, Longin R, Prigent-Combaret C, Dorel C, Hooreman M, Lejeune P. Isolation of an *Escherichia coli* K-12 mutant strain able to form biofilms on inert surfaces: involvement of a new *ompR* allele that increases curli expression. J Bacteriol 1998;180:2442–9.

[11] Johnson JR. Virulence factors in *Escherichia coli* urinary tract infection. Clin Microbiol Rev 1991;4:80–128.

[12] Bauer RJ, Zhang L, Foxman B, et al. Molecular epidemiology of 3 putative virulence genes for *Escherichia coli* urinary tract infection-*usp*, *iha*, and *iroN*(*E. coli*). J Infect Dis 2002;185:1521–4.

[13] Hacker J, Kaper JB. Pathogenicity islands and the evolution of microbes. Annu Rev Microbiol 2000;54:641–79.

[14] Oelschlaeger TA, Dobrindt U, Hacker J. Virulence factors of uropathogens. Curr Opin Urol 2002;12:33–8.

[15] Kanamaru S, Kurazono H, Ishitoya S, et al. Distribution and genetic association of putative uropathogenic virulence factors *iroN*, *iha*, *kpsMT*, *ompT* and *usp* in *Escherichia coli* isolated from urinary tract infections in Japan. J Urol 2003;170:2490–3.

[16] Yamamoto S, Tsukamoto T, Terai A, Kurazono H, Takeda Y, Yoshida O. Distribution of virulence factors in *Escherichia coli* isolated from urine of cystitis patients. Microbiol Immunol 1995;39:401–4.

[17] Terai A, Yamamoto S, Mitsumori K, et al. *Escherichia coli* virulence factors and serotypes in acute bacterial prostatitis. Int J Urol 1997;4:289–94.

[18] Maeyama R, Mizunoe Y, Anderson JM, Tanaka M, Matsuda T. Confocal imaging of biofilm formation process using fluoroprobed *Escherichia coli* and fluoro-stained exopolysaccharide. J Biomed Mater Res A 2004;70:274–82.

[19] Cookson AL, Cooley WA, Woodward MJ. The role of type 1 and curli fimbriae of Shiga toxin-producing *Escherichia coli* in adherence to abiotic surfaces. Int J Med Microbiol 2002;292:195–205.

[20] Genevaux P, Muller S, Bauda P. A rapid screening procedure to identify mini-*Tn10* insertion mutants of *Escherichia coli* K-12 with altered adhesion properties. FEMS Microbiol Lett 1996;142:27–30.

[21] O'Toole GA, Kolter R. Initiation of biofilm formation in *Pseudomonas fluorescens* WCS365 proceeds via multiple, convergent signalling pathways: a genetic analysis. Mol Microbiol 1998;28:449–61.

[22] Schaeffer AJ. Infections of the urinary tract. In: Walsh PC, Retik AB, Vaughan Jr ED, et al., editors. Campbell's urology, vol 1, 8th ed. Philadelphia: Saunders; 2002. p. 515–602.

[23] Nickel JC. Prostatitis and related conditions. In: Walsh PC, Retik AB, Vaughan Jr ED, et al., editors. Campbell's urology, vol 1, 8th ed. Philadelphia: Saunders; 2002. p. 603–30.

Structural and Functional Conversion of Molecular Chaperone ClpB from the Gram-Positive Halophilic Lactic Acid Bacterium *Tetragenococcus halophilus* Mediated by ATP and Stress[▽]

Shinya Sugimoto,[1] Hiroyuki Yoshida,[1] Yoshimitsu Mizunoe,[2] Keigo Tsuruno,[1]
Jiro Nakayama,[1] and Kenji Sonomoto[1,3]*

*Laboratory of Microbial Technology, Division of Microbial Science and Technology, Department of Bioscience and Biotechnology,
Faculty of Agriculture, Graduate School, Kyushu University, 6-10-1 Hakozaki, Higashi-ku, Fukuoka 812-8581, Japan[1];
Department of Bacteriology, Faculty of Medical Sciences, Kyushu University, 3-1-1 Maidashi, Higashi-ku,
Fukuoka 812-8582, Japan[2]; and Laboratory of Functional Food Design, Department of
Functional Metabolic Design, Bio-Architecture Center, Kyushu University,
6-10-1 Hakozaki, Higashi-ku, Fukuoka 812-8581, Japan[3]*

In this study, we report the purification, initial structural characterization, and functional analysis of the molecular chaperone ClpB from the gram-positive, halophilic lactic acid bacterium *Tetragenococcus halophilus*. A recombinant *T. halophilus* ClpB (ClpB$_{Tha}$) was overexpressed in *Escherichia coli* and purified by affinity chromatography, hydroxyapatite chromatography, and gel filtration chromatography. As demonstrated by gel filtration chromatography, chemical cross-linking with glutaraldehyde, and electron microscopy, ClpB$_{Tha}$ forms a homohexameric single-ring structure in the presence of ATP under nonstress conditions. However, under stress conditions, such as high-temperature (>45°C) and high-salt concentrations (>1 M KCl), it dissociated into dimers and monomers, regardless of the presence of ATP. The hexameric ClpB$_{Tha}$ reactivated heat-aggregated proteins dependent upon the DnaK system from *T. halophilus* (KJE$_{Tha}$) and ATP. Interestingly, the mixture of dimer and monomer ClpB$_{Tha}$, which was formed under stress conditions, protected substrate proteins from thermal inactivation and aggregation in a manner similar to those of general molecular chaperones. From these results, we hypothesize that ClpB$_{Tha}$ forms dimers and monomers to function as a holding chaperone under stress conditions, whereas it forms a hexamer ring to function as a disaggregating chaperone in cooperation with KJE$_{Tha}$ and ATP under poststress conditions.

The bacterial heat shock protein ClpB and its eukaryotic homolog HSP104 belong to a class of molecular chaperones whose expressions are strongly induced by various types of stress. The structure and function of ClpB have been well characterized in *Escherichia coli* and *Thermus thermophilus*. ClpB contains two nucleotide-binding domains (NBD1 and NBD2) that are separated by a middle domain forming a coiled-coil structure (1, 2, 17, 31, 34). Moreover, ClpB forms a hexameric single-ring structure and cooperates with the DnaK chaperone system (DnaK, DnaJ, and GrpE; termed KJE) in the solubilization and refolding of aggregated proteins; these reactions are dependent on the presence and hydrolysis of ATP (3, 12, 19, 20, 33). In these reactions, ClpB and KJE may act sequentially or simultaneously. Although the protein dis-aggregation mechanism mediated by the DnaK-ClpB bichaperone system is still under discussion, Bukau and colleagues recently provided direct evidence for the mechanism (26, 32). One study demonstrated that aggregated proteins are solubilized by the continuous extraction of unfolded polypeptides dependent upon the DnaK-ClpB bichaperone system and not

by the fragmentation of large aggregates (26). Here, the middle domain of ClpB is thought to play a crucial role in the initial disaggregation reaction. The other study reported that aggregated proteins are translocated through the central pore of the ClpB hexameric ring and then refolded by KJE (32). However, it was reported that, unlike other chaperones, the ClpB homologs were unable to prevent the aggregation of denatured proteins (11).

In gram-negative bacteria and eukaryotes, the disaggregating activities of ClpB and HSP104 have been reported to be important for resistance to high-temperature stress, cold acclimation, and induced thermotolerance to lethal stress (8, 9, 18, 24). In gram-positive bacteria, a few reports have described the in vivo functions of ClpB: (i) the mutation of *clpB* did not affect the resistance of *Lactococcus lactis* MG1363 to high-temperature, salt, and puromycin stress (13), and (ii) ClpB was required for the induced thermotolerance and virulence of *Listeria monocytogenes* (4). However, the in vitro characterization of ClpB from gram-positive bacteria has yet to be accomplished.

Tetragenococcus halophilus is a moderately halophilic gram-positive lactic acid bacterium with a NaCl optimum of approximately 2 M and an upper limit of approximately 4 M; it is currently exploited in the brewing of Japanese soy sauce (5). In a previous study, we cloned a *dnaK* gene of *T. halophilus* and confirmed that the expression of the *dnaK* gene was induced by salt stress as well as by heat stress (10). Moreover, the in vitro

* Corresponding author. Mailing address: Laboratory of Microbial Technology, Division of Microbial Science and Technology, Department of Bioscience and Biotechnology, Faculty of Agriculture, Graduate School, Kyushu University, 6-10-1 Hakozaki, Higashi-ku, Fukuoka 812-8581, Japan. Phone and fax: 81-(0) 92 642-3019. E-mail: sonomoto@agr.kyushu-u.ac.jp.

TABLE 1. Strains and plasmids used in this study

Strain or plasmid	Characteristic(s)	Reference
Strains		
T. halophilus JCM5888	Wild type	This work
E. coli JM109	recA1 endA1 gyrA96 thi hsdR17 supE44 relA1 (lac-proAB) [F' traD36 proAB⁺ lacIq lacZ M15]	Invitrogen
E. coli BL21(DE3)	F⁻ ompT hsdSB(rB⁻ mB⁻) gal dcm (DE3)	Invitrogen
Plasmids		
pGEM-T easy	Ampʳ, M13ori pBR322ori, linear T overhangs vector	Promega
pET100/D-TOPO	Directional TOPO expression vector; Ampʳ	Invitrogen
pClpB_Tha-M	Partial gene encoding the middle region of T. halophilus ClpB cloned in pGEM-T easy; Ampʳ	This work
pClpB_Tha-N	Partial gene encoding the N-terminal region of T. halophilus ClpB cloned in pGEM-T easy; Ampʳ	This work
pClpB_Tha-C	Partial gene encoding the C-terminal region of T. halophilus ClpB cloned in pGEM-T easy; Ampʳ	This work
pClpB_Tha	T. halophilus clpB gene cloned in pET100/D-TOPO; Ampʳ	This work

and in vivo characterization of the DnaK proteins was also performed under various salinity conditions (28). Because, as mentioned above, DnaK and ClpB are known to form a bichaperone system that efficiently mediates the ATP-dependent reactivation of aggregated proteins, we have a considerable interest in the biochemical properties of ClpB and the DnaK-ClpB bichaperone system in T. halophilus.

In this study, we cloned the clpB (clpB_Tha) gene of T. halophilus and characterized its product overexpressed in E. coli. The purified ClpB_Tha protein formed a hexameric single-ring structure in the presence of ATP and, in cooperation with the T. halophilus DnaK chaperone system (KJE_Tha), reactivated heat-aggregated proteins. Under stress conditions, it dissociated into dimers and monomers, and the resultant low molecular species protected substrate proteins from thermal denaturation and subsequent aggregation. These results provide a novel insight into the structure-function relationship of ClpB under both stress and poststress conditions.

MATERIALS AND METHODS

Bacterial strains and growth conditions. The T. halophilus JCM5888 and E. coli strains used in this study (Table 1) were grown as previously described (10, 28, 29). T. halophilus was grown at 30°C in MRS medium (Oxoid, Hampshire, England) containing 1 M NaCl. E. coli JM109 (Promega, Madison, WI) and BL21 (DE3) (Invitrogen, Carlsbad, CA) were grown at 37°C with shaking in Luria-Bertani (LB) broth. When the growth was appropriate for clonal selection, 5-bromo-4-chloro-3-indolyl-β-D-galactopyranoside (X-Gal), isopropyl-1-thio-β-D-galactopyranoside (IPTG), and ampicillin were added to the culture at concentrations of 50, 40, and 20 μg/ml, respectively.

Cloning of the clpB_Tha gene. Two degenerate oligonucleotide primers, clpB_Tha-ds1 [5'-AA(A/G) TAT CGT GG(T/C) GAA TTT GAA GAA-3'] and clpB_Tha-da1 [5'-(T/C)TT TTC CAT (A/G)TA TTC GGA CAT ATC-3'], used as PCR primers, were designed from the regions conserved among the described ClpB amino acid sequences of gram-positive bacteria, such as Lactococcus lactis subsp. lactis IL1403, Enterococcus faecalis V583, and Streptococcus mutans UA159. PCR was performed using the primers, 1 U of Ex Taq polymerase (Takara, Otsu, Japan), and T. halophilus genomic DNA as a template. The amplified fragment with an expected size of 1.2 kb was cloned into a pGEM-T vector (Promega). The resulting plasmid was named pClpB_Tha-M (Table 1) and sequenced with an ALF express automated DNA sequencer (Amersham Bioscience/GE Healthcare, Uppsala, Sweden).

The regions immediately upstream and downstream of the partial clpB_Tha gene were amplified by inverse PCR (10). The inverse PCR, using NdeI-digested T. halophilus genomic DNA, the primers clpB_Tha-invs1 (5'-GTC GAT GAA GCT TGT GCC AAT ATT CGG GTG-3') and clpB_Tha-inva1 (5'-CTA CCT TCA GTC TTC CCA GCG CCT ACG-3'), and KOD DNA polymerase (Toyobo, Tsuruga, Japan) resulted in a 1,600-bp PCR product containing the sequence 5' to the partial clpB_Tha gene. On the other hand, EcoRI-digested DNA and the primers clpB_Tha-invs2 (5'-CAC CAT GAA TAT TGA AAA AAT GAC AAC CAC ATT ACA-3') and clpB_Tha-inva2 (5'-GGA TCC TTC CTC TTC CAT

TGG TTC ATT AAA G-3') were used to produce an approximate 1,100-bp PCR product that contains the sequence 3' to the partial clpB_Tha gene. The generated fragments were cloned into a pGEM-T vector, and the constructed plasmids were named pClpB_Tha-N and pClpB_Tha-C, respectively (Table 1). The sequences obtained were analyzed with GENETYX-WIN (Software Development, Tokyo, Japan). The free energy of the stem-loop structure was also calculated with this software.

Nucleotide sequence accession numbers. The nucleotide sequence of T. halophilus JCM5888 clpB that was determined in this study has been registered in the EMBL, GenBank, and DDBJ databases under accession number AB239684.

Plasmid construction and overexpression of ClpB_Tha in E. coli. The gene encoding ClpB_Tha was PCR amplified from T. halophilus genomic DNA with two oligonucleotide primers, ClpB_Tha-s1 (5'-CAC CAT GAA TAT TGA AAA AAT GAC AAC CAC ATT ACA-3') and ClpB_Tha-a1 (5'-GGA TCC TTC CTC TTC CAT TGG TTC ATT AAA G-3'). The amplified fragment was cloned into an E. coli expression vector, pET-100/D-TOPO (Invitrogen), according to the manufacturer's instructions. The vector pET-100/D-TOPO carried a His₆ tag, which was thus incorporated in the protein at the N terminus of the clpB_Tha gene product. The constructed plasmid, named pClpB_Tha (Table 1), was transformed into E. coli BL21(DE3). The overexpression of ClpB_Tha was performed as previously reported (10, 28, 29). The E. coli cells were grown to an optical density at 600 nm in LB medium containing 50 μg/ml ampicillin at 37°C of 0.5, and then IPTG was added to a concentration of 1 mM. After a further 3 h at 37°C, the cells were harvested by centrifugation and stored at −80°C.

Purification of the ClpB_Tha protein. The ClpB_Tha protein containing the His₆ tag was purified by nickel affinity chromatography (10, 28, 29). Since the ClpB_Tha purified by nickel affinity chromatography contained some impurities, both hydroxyapatite chromatography and gel filtration chromatography were used as additional purification steps. The fractions containing ClpB_Tha were dialyzed against 20 mM sodium phosphate buffer (pH 6.8) with a Slide-A-Lyzer cassette (Pierce, Rockford, IL) and then concentrated by ultrafiltration with an Amicon Ultra-30 centrifugal filter device (30-kDa cutoff) (Millipore, Bedford, MA). The concentrated proteins were further purified using a hydroxyapatite CHT5-1 column (Bio-Rad, Tokyo, Japan) equilibrated with 20 mM sodium phosphate buffer (pH 6.8). The proteins were eluted with a 100 ml linear gradient of 20 to 500 mM sodium phosphate (pH 6.8). Fractions containing ClpB_Tha were then applied to a COSMOSIL 5Diol-300-II gel filtration column (Nacalai Tesque, Kyoto, Japan) equilibrated with 20 mM sodium phosphate buffer (pH 6.8) containing 100 mM sodium sulfate. The column was developed by the same buffer at a flow rate of 0.5 ml/min and monitored by absorbance at 280 nm. The fractions containing ClpB_Tha were collected and concentrated by ultrafiltration. After gel filtration chromatography, a highly pure ClpB_Tha was yielded, running as a single band on a sodium dodecyl sulfate (SDS)-polyacrylamide gel (data not shown). The protein concentrations were determined by using a Bradford assay kit (Nacalai Tesque) with bovine serum albumin (BSA; Sigma, St. Louis, MO) as a standard. If not otherwise indicated, the molar concentrations for all the proteins given in the text refer to the respective monomers.

Protease sensitivity assay. Prior to the addition of trypsin, 10 μl of purified ClpB_Tha protein (1 μM) was preincubated in Tris-HCl buffer (pH 7.4) containing 100 mM KCl, 20 mM MgCl₂, and 1 mM dithiothreitol (DTT) for 10 min on ice with and without 5 mM ATP or ADP. Trypsin (Sigma) was then added to the reaction mixtures to a final concentration of 10 ng/μl, and the mixtures were incubated at 37°C. At the indicated incubation time (from 0 to 60 min), the reactions were quenched by the addition of 5 μl of SDS-polyacrylamide gel

electrophoresis (PAGE) sample buffer containing Tris-HCl (pH 8.0), glycerol, 1% (wt/vol) 2-mercaptoethanol, 1% (wt/vol) SDS, and 0.1% (wt/vol) bromophenol blue. Samples were separated by electrophoresis using 12% SDS-polyacrylamide gels. The gels were stained with Coomassie brilliant blue (CBB) R-250 (Nacalai Tesque).

Gel filtration chromatography analysis. Twenty-five micromolar purified ClpB$_{Tha}$ protein was incubated for 10 min on ice with or without 2 mM ATP, pH 7.4. The samples (50 μl) were centrifuged at 4°C for 15 min before loading onto a TSK G4000SW$_{XL}$ gel filtration column (Tosoh, Tokyo, Japan). The column was developed with 50 mM Tris-HCl buffer (pH 7.4) containing 100 mM KCl, 20 mM MgCl$_2$, 1 mM DTT, and 2 mM ATP (if required), with a flow rate of 0.5 ml/min, and monitored by absorbance at 290 nm.

The apparent molecular masses of ClpB$_{Tha}$ proteins, including thyroglobulin (669,000 Da), apoferritin (440,000 Da), alcohol dehydrogenase (150,000 Da), and BSA (66,000 Da), were calculated using a molecular weight standard kit (Sigma).

Chemical cross-linking. The purified ClpB$_{Tha}$ protein was dialyzed against 50 mM Tris-HCl (pH 7.4) containing 100 mM KCl, 20 mM MgCl$_2$, and 1 mM DTT. Forty-microliter samples (2.5 μM) were incubated on ice for 1 h after the addition of 5 mM ATP, ADP, AMP, or adenosine 5'-O-(thiotriphosphate) (ATPγS), a nonhydrolyzable ATP analog. Cross-linking was initiated by the addition of 0.1% glutaraldehyde and terminated by the addition of 10 μl of SDS-PAGE sample buffer after incubation at 30°C for 20 min. The samples were boiled for 5 min and resolved by electrophoresis on a 3 to 10% SDS-polyacrylamide gradient gel. The gels were stained with CBB R-250.

Electron microscopy. The molecular shape of the ClpB$_{Tha}$ was examined by negative staining using 0.5% uranyl acetate in a JEM 2000EX electron microscope (JEOL, Tokyo, Japan) at 100 kV (29). Since the ATP-induced oligomer was unstable and readily dissociated during the preparation of samples for electron microscopy, the oligomer was cross-linked with 0.1% glutaraldehyde.

Reactivation of heat-inactivated protein. One micromolar lactate dehydrogenase (LDH) from *Leuconostoc mesenteroides* (Oriental Yeast, Osaka, Japan) was thermally denatured at 50°C for 15 min. The denatured LDH protein was divided into soluble and insoluble fractions by centrifugation at 20,000 × g for 30 min, and each fraction was analyzed by SDS-PAGE. Since LDH was detected in only the insoluble fraction, the heat-treated LDH was used as an aggregated protein substrate. Aggregated LDH was diluted 10-fold with 50 mM Tris-HCl buffer (pH 7.4) containing 100 mM KCl, 20 mM MgCl$_2$, and 1 mM DTT in the presence or absence of KJE$_{Tha}$ (DnaK, 2 μM/DnaJ, 0.5 μM/GrpE, 0.25 μM), ClpB$_{Tha}$ (2 μM), and ATP (5 mM) and was incubated at 30°C. Aliquots were taken up at different time points and tested for LDH activity.

Prevention of the denaturation and aggregation of substrate proteins. LDH (100 nM) was incubated at 45°C in 50 mM Tris-HCl buffer (pH 7.4) containing 100 mM KCl, 20 mM MgCl$_2$, and 1 mM DTT in the presence or absence of ClpB$_{Tha}$ (0.5 μM). Aliquots were withdrawn at different time points and tested for residual LDH activity at 30°C as previously described (28). The activity measured just before heating was defined as 100%. BSA (1 μM) was used instead of ClpB$_{Tha}$ as a control.

Yeast enolase (1 μM, Sigma) was incubated at 50°C for 1 h in 50 mM Tris-HCl buffer (pH 7.4) containing 20 mM KCl, 10 mM Mg acetate, and 2 mM DTT, in the presence or absence of ClpB$_{Tha}$ (0.5 μM). After incubation, samples were centrifuged at 20,000 × g for 30 min and divided into soluble and insoluble fractions. Each fraction was analyzed by 12% SDS-PAGE.

E. coli proteins (1.5 mg/ml) were incubated at 50°C in 50 mM Tris-HCl buffer (pH 7.4) containing 100 mM KCl, 20 mM MgCl$_2$, and 1 mM DTT in the presence or absence of ClpB$_{Tha}$ (0.5 μM). Aggregation was monitored for 10 min as the increase in absorbance at 320 nm.

RESULTS

Cloning and nucleotide sequence analysis of the *clpB* locus in *T. halophilus* JCM5888. The highly conserved amino acid sequences of the ClpB proteins from *L. lactis* subsp. *lactis* IL-1403, *E. faecalis* V583, and *S. mutans* UA159 were used to construct the degenerative primers for the identification of a putative *clpB* gene in the *T. halophilus* JCM5888 genome. In this way, a single open reading frame encoding an 872-amino-acid protein with a predicted molecular mass of 98,536 Da was identified. The protein exhibits high similarities to the ClpB proteins from a wide variety of bacteria, and the highest sim-

ilarity (84.4%) is to that from *E. faecalis*. Upstream of *clpB*, a putative promoter region was found with a −35 sequence, 5'-TTAACA-3', and a −10 sequence, 5'-TATAC-3'. On the other hand, a deduced rho-independent transcriptional terminator region, which had a free energy of −34.5 kcal · mol^{-1}, was identified immediately downstream of *clpB*. By comparing putative regulatory elements for *clpB* genes from various gram-positive bacteria, we identified a putative CtsR binding site in the *clpB* locus from *T. halophilus*. CtsR is a negative regulator of class III heat shock genes and is proposed to bind to a consensus sequence containing a direct repeat hepta-nucleotide sequence separated by three nucleotides: A/*GGTCAAA*N AN*A/GGTCAAA* (6), where the italic type indicates a direct repeat. The CtsR binding site located on the *clpB* gene of *T. halophilus* overlapped with the −35 promoter region and had an orientation inverse to that of the consensus sequence, *TTT GACCAATTTTGACC* (where the italic type indicates a direct repeat), similar to that of *L. lactis clpB* and *clpP* (30). These results suggest that the expression of the *clpB*$_{Tha}$ gene is regulated by CtsR in a manner similar to those of other gram-positive bacteria.

The amino acid alignment with various bacterial ClpBs demonstrated that ClpB$_{Tha}$ possesses two NBD, NBD1 (amino acids 183 to 409) and NDB2 (amino acids 548 to 729), each harboring both Walker A and B motifs characterized by Walker-type ATPase (data not shown). The two NBDs are separated by a spacer-middle domain of 139 amino acids (410 to 547) that has the potential to form a coiled-coil structure.

Nucleotide-induced oligomerization of ClpB$_{Tha}$. The ClpB homologs are known to undergo conformational changes following the addition of ATP (1, 2, 17, 22, 31, 34). In order to obtain similar information for ClpB$_{Tha}$, we examined the effect of ATP on the conformational changes of ClpB$_{Tha}$ by means of protease digestion. ClpB$_{Tha}$ was incubated in the presence and absence of ATP or ADP for several minutes at 37°C and then analyzed by SDS-PAGE. In the absence of nucleotides, ClpB$_{Tha}$ was digested into several 30- to 70-kDa fragments and the amount of intact ClpB$_{Tha}$ was significantly decreased, as shown in Fig. 1A. In the presence of ATP or ADP, ClpB$_{Tha}$ was relatively protected and a large proportion of the ClpB$_{Tha}$ remained intact. These results indicate that ClpB$_{Tha}$ undergoes conformational changes in the presence of ATP or ADP.

In order to determine whether the changes in the proteolytic sensitivity of ClpB$_{Tha}$ are due to changes in the oligomeric states, the purified ClpB$_{Tha}$ was subjected to analytical gel filtration chromatography by using a TSK G4000SW$_{XL}$ column in the presence or absence of ATP. In the absence of ATP, ClpB$_{Tha}$ was eluted at the position of a 200-kDa standard (Fig. 1B) and the peak was tailed. Thus, in the absence of ATP, ClpB$_{Tha}$ forms both dimers and monomers. In the presence of ATP in the running buffer, the elution position of ClpB$_{Tha}$ was shifted dramatically and slightly behind a 669-kDa standard, indicating that ClpB$_{Tha}$ apparently forms a hexamer in the presence of ATP (Fig. 1B). In the absence of ATP in the running buffer, a preincubated ClpB$_{Tha}$ with ATP was also analyzed by analytical gel filtration chromatography. ClpB$_{Tha}$ was eluted at the position of ca. 200 kDa with a long tail, and the bound ATP was released from ClpB$_{Tha}$ inside the column (data not shown); this suggests that the ClpB$_{Tha}$ hexamer dis-
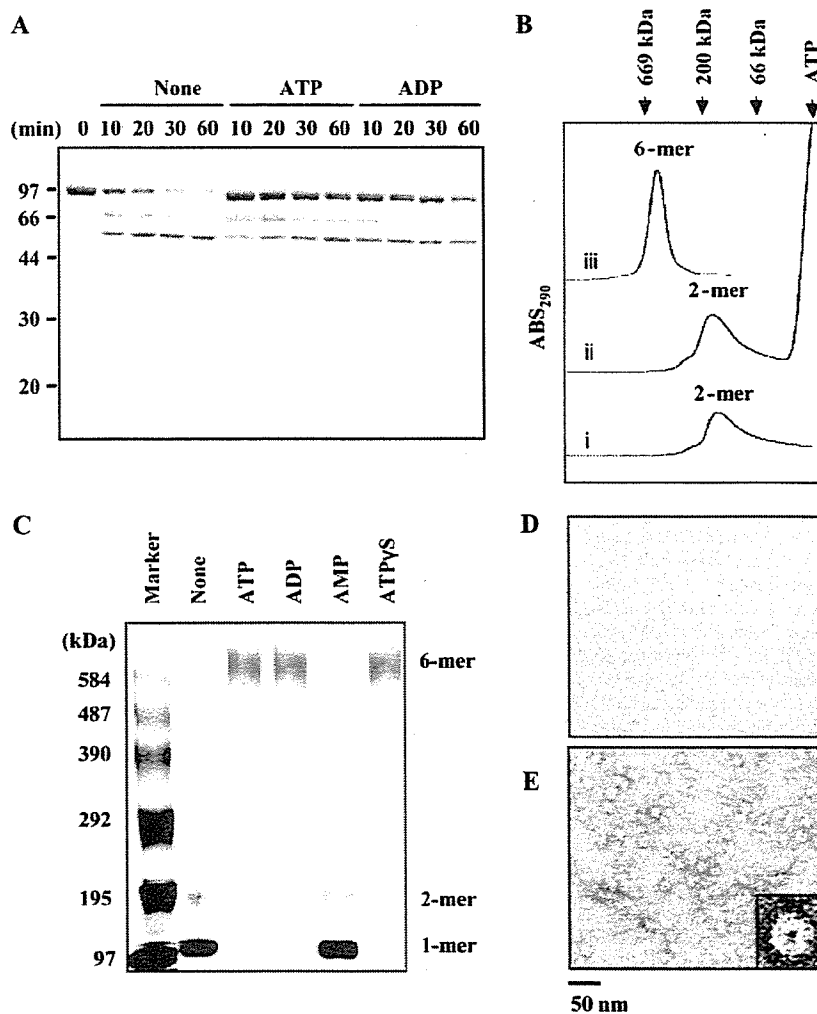
FIG. 1. Effect of nucleotides on the conformational change of ClpB$_{Tha}$. (A) Proteolytic sensitivity of ClpB$_{Tha}$ in the presence and absence of ATP or ADP. Ten microliters of purified ClpB$_{Tha}$ (1 μM) was incubated at 37°C for the indicated periods with 100 ng of trypsin either in the presence or absence of 5 mM ATP or ADP. The resultant fragments were separated by electrophoresis with a 12% SDS-polyacrylamide gel and stained by CBB R-250. The numbered bars to the left of the figure indicate the migration positions of molecular mass markers in kilodaltons. (B) The oligomerization of ClpB$_{Tha}$ was analyzed by gel filtration chromatography. Samples (25 μM) were preincubated without (i) or with (ii) 2 mM ATP and subjected to gel filtration chromatography by using the running buffer without ATP. Sample preincubated without ATP was also subjected to gel filtration chromatography using the running buffer with 2 mM ATP (iii). In all cases, elution was monitored by the absorbance at 290 nm (ABS$_{290}$). (C) The oligomeric structure of ClpB$_{Tha}$ was analyzed by cross-linking. ClpB$_{Tha}$ (2.5 μM) was cross-linked at 30°C with 0.1% glutaraldehyde for 20 min in the presence and the absence of 5 mM indicated nucleotides. Cross-linking reaction was terminated by the addition of SDS-PAGE sample buffer. Samples were resolved by electrophoresis on a 3 to 10% SDS-polyacrylamide gradient gel. The gels were stained with CBB R-250. Cross-linked phosphorylase B proteins (Sigma) were also resolved as a high-molecular-weight marker. (D) ClpB$_{Tha}$ (2.5 μM) was incubated in the absence of ATP on ice for 1 h and cross-linked with 0.1% glutaraldehyde for 20 min. The cross-linking reaction was terminated by the addition of 1 M glycine. Oligomeric structure was visualized by electron microscopy. (E) Oligomeric structure of ClpB$_{Tha}$ in the presence of 5 mM ATP was also analyzed by electron microscopy as described in Fig. 1D.

sociates into dimers and monomers under conditions of ATP depletion.

Since mobility in gel filtration chromatography is often influenced by the shape of the protein, cross-linking procedures were used as an alternative method to examine the oligomeric state of ClpB$_{Tha}$ on an SDS polyacrylamide gel (Fig. 1C). The cross-linked monomer band migrated rapidly compared to the non-cross-linked one; this is probably a consequence of the intramolecular cross-linking described previously (22). The ClpB$_{Tha}$ cross-linked in the absence of ATP revealed two bands corresponding to dimer (ca. 200 kDa) and monomer (ca.

100 kDa) subunits. On the other hand, the subunits of ClpB$_{Tha}$ are cross-linked to form a hexamer (ca. 600 kDa) in the presence of ATP. Under these conditions, other oligomers, such as heptamers and pentamers, were not detected. We also examined the effects of ADP, AMP, and ATPγS (a nonhydrolyzable ATP analog) on hexamer formation. ADP and ATPγS induced hexamerization, whereas AMP did not.

In order to further analyze the oligomeric structure of ClpB$_{Tha}$, we performed electron microscopy analysis using a purified protein after cross-linking reactions in the presence or absence of ATP. The electron micrograph of the negatively
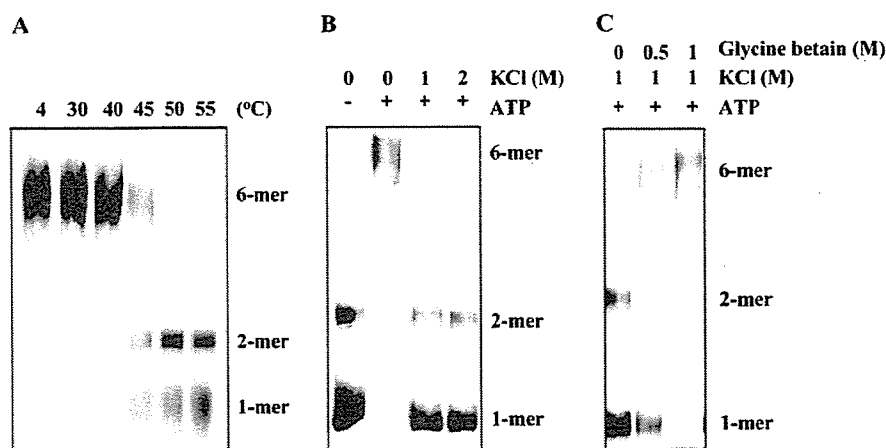
FIG. 2. Effects of temperature and salt concentration on the conformational change of ClpB$_{Tha}$. (A) Effects of temperature on the oligomeric state of ClpB$_{Tha}$ were analyzed by cross-linking experiment. Samples (2.5 μM) were incubated at the indicated temperatures in the presence of 5 mM ATP for 30 min before cross-linking reaction. Cross-linking reaction and SDS-PAGE analysis were carried out as described in the legend for Fig. 1C. (B) Effects of salt concentration on the oligomeric state of ClpB$_{Tha}$ were analyzed by a cross-linking experiment. Samples (2.5 μM) were incubated at 30°C for 1 h in the presence of 5 mM ATP and the indicated concentrations of KCl before cross-linking reaction. Cross-linking reaction and analysis were carried out as described in the legend for Fig. 1C. −, absence of; +, presence of. (C) Effect of glycine betaine on the ATP-induced oligomerization of ClpB$_{Tha}$ under high-salinity conditions was analyzed by a cross-linking experiment. Samples (2.5 μM) were incubated at 30°C for 1 h in the presence of 5 mM ATP, 1 M KCl, and the indicated concentrations of glycine betaine before cross-linking reaction. Cross-linking reaction and analysis were carried out as described in the legend for Fig. 1C. +, presence of.

stained ClpB$_{Tha}$ in the absence of ATP exhibited small amorphous particles as shown in Fig. 1D, while that in the presence of ATP revealed ring-shaped structures (Fig. 1E); this is consistent with the observations of other bacterial and eukaryotic ClpB homologs (1, 2, 14, 17, 31, 34). Although the resolution of the electron micrograph was not sufficiently high to determine the number of subunits, taking into consideration the sequence similarity of the protein to those characterized in other bacterial systems and the abovementioned results of gel filtration chromatography and the cross-linking experiment (Fig. 1B and C), it is highly likely that the ClpB$_{Tha}$ was assembled into a hexamer in the presence of ATP or ADP.

Taken together, these observations suggest that the binding of ATP or ADP is involved in the hexamerization of ClpB$_{Tha}$ and the removal of these molecules results in the dissociation of the complex into dimeric and monomeric structures.

Effects of temperature and salt concentration on the ATP-induced hexamerization of ClpB$_{Tha}$. The oligomeric structures of ClpB homologs have often been analyzed under nonstress conditions (1, 2, 14, 17, 31, 34); however, to date, little is known about these structures under stress conditions. To address this issue, we examined the effects of temperature and salt concentration on the stability of the ATP-induced ClpB$_{Tha}$ hexamer by a cross-linking procedure.

Figure 2A shows the effects of temperature on the hexamerization of ClpB$_{Tha}$. After 30 min of cooling at 4°C or heat treatment at 30°C and 40°C in the presence of ATP, a single band corresponding to the hexamer was detected. On the other hand, the intensity of the hexamer band decreased and low molecular bands, indicating dimer and monomer subunits, appeared after an incubation at 45°C, even in the presence of ATP. At temperatures of 50°C or more, the ATP-induced hexamer was completely dissociated into dimers and monomers; similar dissociation was also observed in the case of the

ADP-induced hexamer (data not shown). ClpB$_{Tha}$ remained folded at 55°C, which was confirmed by circular dichroism spectra measurements (data not shown), indicating that heat stress at 45°C or more did not change the secondary structure of ClpB$_{Tha}$; however, heat stress does dissociate an ATP-induced hexamer into dimers and monomers.

Figure 2B shows the effects of salt concentration on the ATP-induced hexamerization of ClpB$_{Tha}$. Because it has been reported (23) that T. halophilus accumulates high concentrations of potassium ions, more than 1 M in the cell, we examined the effects of 1 to 2 M KCl on the oligomeric state of ClpB$_{Tha}$. In the presence of KCl at the concentrations of 1 M or more, regardless of the presence of ATP, a hexameric structure could not be detected, while dimeric and monomeric structures became predominant (Fig. 2B). Similar dissociations were observed in the presence of 1 M NaCl instead of KCl and in the case of the ADP-induced hexamer (data not shown). The results of the circular dichroism spectra analysis demonstrated that ClpB$_{Tha}$ was not unfolded even at high concentrations of KCl beyond 1 M (data not shown).

Since T. halophilus accumulates large amounts of compatible solutes as well as potassium ions when grown in medium containing such organic compounds (23), we analyzed the effects of glycine betaine, a known compatible solute, on the oligomerization of ClpB$_{Tha}$ (Fig. 2C). Although, as mentioned above, high concentrations of KCl dissociated the ATP-induced hexamer, glycine betaine counterbalanced the dissociation effect. Glycine betaine at a concentration of 1 M completely stabilized the ATP-induced hexamer, even in the presence of 1 M KCl. These results indicate that charge screening is responsible for the change in quaternary structure and that such changes can be prevented by the presence of glycine betaine.

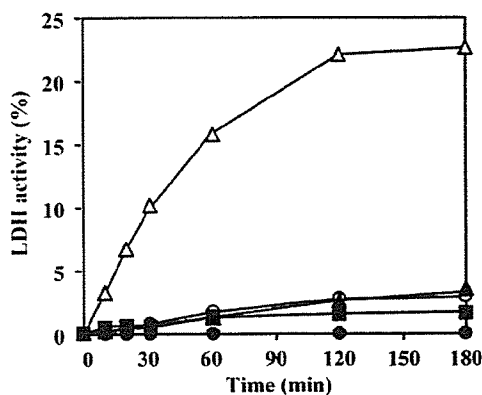Gel filtration analysis was also conducted to verify the results

FIG. 3. Disaggregation activity of ClpB$_{Tha}$ in cooperation with KJE$_{Tha}$. Thermal aggregated LDH (100 nM) was incubated at 30°C with the following chaperone sets: no chaperones (closed circles), KJE$_{Tha}$ alone (DnaK, 2 μM/DnaJ, 0.5 μM/GrpE, 0.25 μM) (open circles), ClpB$_{Tha}$ (2 μM) alone (closed triangles), ClpB$_{Tha}$ with KJE$_{Tha}$ and 5 mM ATP (open triangles), and ClpB$_{Tha}$ with KJE$_{Tha}$ and no ATP (closed squares). Aliquots were taken up at different time points and tested for LDH activity. The activity of native LDH before thermal treatment was defined as 100%.

of the cross-linking (Fig. 2) and showed that the ClpB$_{Tha}$ oligomer was dissociated at 50°C or in the presence of 0.5 M KCl; its status was not affected at various protein concentrations ranging from 2.5 to 20 μM (data not shown). Therefore, we conclude that the ATP-induced hexamer dissociates into dimers and monomers under heat stress or salt stress (without glycine betaine) conditions.

Renaturation of heat-aggregated proteins by the DnaK-ClpB bichaperone system. The hexameric ClpB homologs have been well characterized and have been demonstrated to cooperate with the DnaK system (KJE) in the solubilization and reactivation of aggregated proteins (3, 12, 19, 20, 33). In order to confirm whether ClpB$_{Tha}$ possesses the ClpB-specific disaggregation activity, we performed a reactivation assay using heat-aggregated LDH as a substrate protein (Fig. 3). The LDH activity was not recovered spontaneously. KJE$_{Tha}$ or ClpB$_{Tha}$ alone exhibited very little recovery of activity. Only when incubated in the presence of both KJE$_{Tha}$ and ClpB$_{Tha}$ was the aggregated LDH significantly renatured; its activity reached 23% of the initial value after a 3-h incubation at 30°C. However, the recovery of LDH activity by the DnaK$_{Tha}$-ClpB bichaperone system was not observed in the absence of ATP. These results indicate that ClpB$_{Tha}$ forms a hexamer in the presence of ATP and, in cooperation with KJE$_{Tha}$, reactivates aggregated proteins. Here, we demonstrate that ATP is required for both the hexamerization of ClpB$_{Tha}$ and the disaggregation activity of the bichaperone system.

Effect of ClpB$_{Tha}$ on the denaturation and aggregation of substrate proteins. In order to assess the intrinsic chaperone activities of the dimeric and monomeric ClpB$_{Tha}$, which to date have not been reported in ClpB homologs, we tested the protection of LDH from thermal inactivation in vitro. BSA, known as a protective agent for enzymes, did not significantly protect LDH from thermal inactivation at 45°C (Fig. 4A). On the contrary, ClpB$_{Tha}$ remarkably suppressed the inactivation in the absence of ATP, suggesting that the dimers and monomers
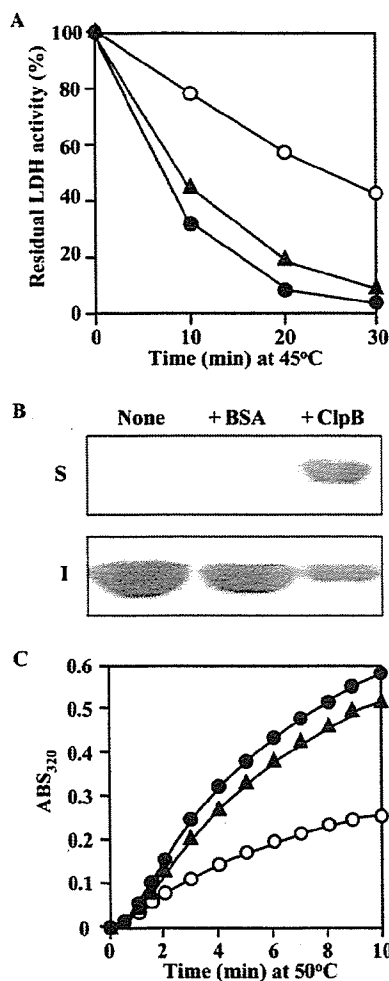

FIG. 4. General chaperone activity of ClpB$_{Tha}$. Each substrate protein (LDH, 100 nM; enolase, 1 μM; *E. coli* proteins, 1.5 mg/ml) was incubated at the indicated temperatures in either the absence (closed circles) or the presence of ClpB$_{Tha}$ (0.5 μM) (open circles). BSA (1 μM) was used instead of ClpB$_{Tha}$ as a control (closed triangles). (A) Thermal inactivation of LDH at 45°C was analyzed. At the indicated time points, LDH activity at 30°C was measured. The *y* axis shows the relative activity in which the initial LDH activity was defined as 100% activity. (B) Heat-induced aggregation of enolase was analyzed by SDS-PAGE. Samples incubated at 50°C for 1 h were divided into soluble (S) and insoluble (I) fractions by centrifugation (20,000 × *g* for 30 min). Each fraction was analyzed by 12% SDS-PAGE. +, presence of. (C) Heat-induced aggregation of proteins extracted from *E. coli* at 50°C was measured as a function of absorbance at 320 nm.

of ClpB$_{Tha}$ protect the proteins from irreversible denaturation leading to aggregation.

We then tested the suppression of substrate thermal aggregation using enolase as a substrate. Enolase was incubated at 50°C for 1 h and then separated into supernatant and precipitate fractions by centrifugation; each fraction was analyzed by SDS-PAGE (Fig. 4B). When enolase was incubated alone or with BSA, it formed large aggregates and was precipitated. Incubation of enolase with ClpB$_{Tha}$ in the absence of ATP resulted in the decrease of aggregated enolase and, consequently, large amounts of enolase remained in the soluble fraction. Since we speculated that the effect of ClpB$_{Tha}$ on the

thermal aggregation of enolase might be specific for this enzyme, we used proteins extracted from *E. coli* as an alternative substrate (Fig. 4C). The extracted proteins were incubated at 50°C, and the aggregation was monitored by measuring the absorbance at 320 nm, the wavelength usually used for monitoring the aggregation of proteins (16, 27). When the *E. coli*-extracted proteins were incubated alone or with BSA, the absorbance increased gradually. On the other hand, the rate of aggregation and the maximum absorbance value at 320 nm within 10 min in the presence of ClpB$_{Tha}$ were lower than those in the absence of it. These results indicate that dimer- and monomer-forming ClpB$_{Tha}$ in the absence of ATP suppresses the thermal aggregation of the substrate proteins and that it possesses general chaperone activities.

DISCUSSION

Until now, the biochemical characterization of ClpB homologs has been conducted to determine their structures and functions (1–3, 17, 19, 20, 31, 33, 34). Despite the fact that these molecules are required for resistance to high-temperature stress, cold acclimation, and induced thermotolerance to lethal stress (8, 9, 18, 24), these in vitro studies were performed mostly under nonstress conditions. Moreover, unlike gram-negative bacteria and eukaryotes, little is known about the structure and function of gram-positive bacterial ClpBs; this is despite the fact that, with the exception of *Bacillus subtilis*, these molecules are carried on the genomes of all gram-positive bacteria (21). In this report, we described a novel aspect of the ClpB from the gram-positive halophilic lactic acid bacterium *T. halophilus*, that is, a structural and functional conversion mediated by ATP and stress.

As demonstrated by gel filtration chromatography, chemical cross-linking with glutaraldehyde, and electron microscopy, ClpB$_{Tha}$ formed a hexameric single-ring structure in the presence of ATP, ADP, and ATPγS, while it existed as dimeric and monomeric structures in the absence of them (Fig. 1). Considering that ClpB$_{Tha}$ did not hydrolyze ADP (data not shown) and that ATPγS induced hexamerization, nucleotide binding, but not its hydrolysis, was required for hexamer formation, as in the case of other characterized bacterial ClpBs (1, 14, 31, 34). Although the overall ring structure of the oligomer in the presence of ATP appears to be conserved among bacterial ClpB homologs, the effects of ADP on their oligomerization appears to differ among species. *Saccharomyces cerevisiae* HSP104 (22, 25) and *S. cerevisiae* mitochondrial HSP78 (15), the most closely related to ClpB and HSP104, formed hexamers in the presence of ADP similar to ClpB$_{Tha}$ (Fig. 1). On the other hand, *E. coli* ClpB and *T. thermophilus* ClpB formed small oligomers (2- to ~5-mer) but not a hexamer in the presence of ADP (31, 34). Moreover, the oligomeric states of ClpB homologs in the absence of nucleotides also differ among species. *T. thermophilus* ClpB formed small oligomers (~5-mer) in the absence of nucleotides, while *S. cerevisiae* HSP104 and mitochondrial HSP78 formed monomers (15, 22). Interestingly, *E. coli* ClpB formed a heptamer in the absence of nucleotides and a hexamer in the presence of ATP; therefore, the binding of ATP induces a change in the self-association state of *E. coli* ClpB from that of a heptamer to that of a hexamer (1, 14). ClpB$_{Tha}$ differs from those aforementioned in
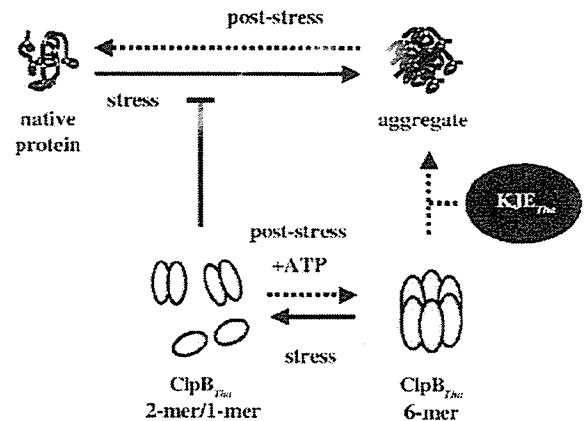

FIG. 5. Model for structural and functional conversion of ClpB$_{Tha}$ mediated by ATP and stress. Under stress conditions, including heat stress and salt stress, unstable intracellular proteins are easily denatured and aggregated. Under these conditions, ClpB$_{Tha}$ forms dimeric and monomeric structures which are able to suppress aggregation of labile proteins as a first defense mechanism (solid line). On the other hand, under poststress conditions, ClpB$_{Tha}$ forms a hexameric ring structure depending upon the presence of ATP (dotted line). In cooperation with KJE$_{Tha}$, the hexameric ClpB$_{Tha}$ can reactivate preexisting aggregates as a second defense mechanism (dotted line).

that it exists as a mixture of dimers and monomers (Fig. 1). Nonetheless, the hexameric ring structure of the ClpB homologs, which is believed to be the functional structure, is widely conserved from prokaryotes to eukaryotes.

Previously, the effect of temperature on the oligomerization of ClpB had been demonstrated only in *T. thermophilus* (31). *T. thermophilus* ClpB formed small oligomers (~5-mer) in the presence of ATP at 20°C, a much lower temperature than the physiological temperature for the host, while it formed a hexamer at 55°C, a temperature at which *T. thermophilus* ClpB is active as a molecular chaperone. This implies that an increase in temperature stabilizes the hexamer of *T. thermophilus* ClpB (31). In contrast, an increase in temperature in excess of 45°C, which is considered as a sublethal temperature for *T. halophilus* (10), destabilized the hexameric structure of ClpB$_{Tha}$ (Fig. 2A). To our knowledge, this is the first report that describes the oligomeric structure of ClpB homologs under heat stress conditions.

The effects of high concentrations of salts on the oligomerization of ClpB homologs were also previously reported (7, 14, 25, 31). Their oligomers were destabilized when the KCl and NaCl concentrations were increased. However, the effects of these salts were counterbalanced by the presence of ATP. Surprisingly, as demonstrated by cross-linking under high-salinity conditions, ClpB$_{Tha}$ formed both dimers and monomers, even in the presence of ATP (Fig. 2B). It is notable that the intracellular concentrations of potassium ions in *T. halophilus* can accumulate to levels in excess of 1 M (23). Can ClpB$_{Tha}$ form hexamers in vivo under such high-salinity conditions? To address this question, we then analyzed the effect of glycine betaine on the oligomerization of ClpB$_{Tha}$ in the presence of ATP and 1 M KCl. The results demonstrated that glycine betaine counterbalanced the dissociation effect of salt (Fig. 2C), suggesting that in vivo ClpB$_{Tha}$ can form a hexamer in the presence of ATP. However, an excess amount of KCl com-

pared to glycine betaine induced the dissociation of the hexamer. Moreover, there was no effect of glycine betaine on the structural change of ClpB$_{Tha}$ under heat stress conditions (Fig. 5). Taken together, our observations indicate that the ATP-induced oligomerization of ClpB$_{Tha}$ was affected by the surrounding environmental conditions, such as a high temperature and the salt concentration.

Disaggregation activities are widely conserved among the ClpB homologs. In fact, ClpB$_{Tha}$ also reactivated heat-aggregated LDH in an ATP-dependent cooperation with the DnaK$_{Tha}$ system (Fig. 3). Interestingly, ClpB$_{Tha}$ exhibited general chaperone activities, such as the protection of substrates from both thermal inactivation and aggregation, in the absence of ATP (Fig. 4). Under these conditions, as demonstrated by cross-linking (Fig. 2A), ClpB$_{Tha}$ formed dimers and monomers. After the dissociation of the hexamer into dimers and monomers, these species appear to expose the hydrophobic regions and substrate binding sites hidden inside the ring; this might enable the molecules to interact with unfolded proteins. This behavior may be similar to that of other chaperones, including the DnaK and GroEL systems. Why, nevertheless, does ClpB$_{Tha}$ possess intrinsic chaperone activities? One possible explanation is that ClpB$_{Tha}$ compensates for the impaired function of the DnaK$_{Tha}$ system whose in vitro chaperone activity is lower than that of the *E. coli* system (S. Sugimoto et al., unpublished data). The independent and/or cooperative functions of the ClpB$_{Tha}$ and DnaK$_{Tha}$ systems are now under investigation in vivo.

Based on the results presented in this study, we propose the following model for the structural and functional conversion of ClpB$_{Tha}$ (data not shown). Under stress conditions, particularly at high temperatures, intracellular labile proteins might be easily denatured and form aggregates. Accumulations of large amounts of these aggregates and the loss of active proteins, including several essential for cell growth, have toxic effects on the host cells (32). Under these types of stress conditions, ClpB$_{Tha}$ forms dimer and monomer structures and these protect substrate proteins from aggregation by binding to unfolded proteins and by suppressing the formation of aggregates. This facilitates a rapid first defense against stress, including heat and salt stress. Under poststress conditions, aggregates formed in response to stress would be repaired by the DnaK-ClpB bichaperone system, where ClpB$_{Tha}$ forms hexameric ring structure depending on the presence of ATP.

To our knowledge, this is the first report to describe the functional conversion of the molecular chaperone ClpB associated with a structural change. Further investigations will be required to determine whether this property is common among gram-positive bacteria and some other organisms; these investigations may provide us with a unique insight into the role of molecular chaperone systems.

ACKNOWLEDGMENTS

REFERENCES

1. Akoev, V., E. P. Gogol, M. E. Barnett, and M. Zolkiewski. 2004. Nucleotide-induced switch in oligomerization of the AAA$^+$ ATPase ClpB. Protein Sci. 13:567–574.
2. Barnett, M. E., A. Zolkiewska, and M. Zolkiewski. 2000. Structure and activity of ClpB from *Escherichia coli*. Role of the amino- and carboxyl-terminal domains. J. Biol. Chem. 275:37565–37571.
3. Beinker, P., S. Schlee, Y. Groemping, R. Seidel, and J. Reinstein. 2002. The N terminus of ClpB from *Thermus thermophilus* is not essential for the chaperone activity. J. Biol. Chem. 277:47160–47166.
4. Chastanet, A., I. Derré, S. Nair, and T. Msadek. 2004. *clpB*, a novel member of the *Listeria monocytogenes* CtsR regulon, is involved in virulence but not in general stress tolerance. J. Bacteriol. 186:1165–1174.
5. Collins, M. D., A. M. Williams, and S. Wallbanks. 1990. The phylogeny of *Aerococcus* and *Pediococcus* as determined by 16S rRNA sequence analysis: description of *Tetragenococcus* gen. nov. FEMS Microbiol. Lett. 70:255–262.
6. Derré, I, G. Rapoport, and T. Msadek. 1999. CtsR, a novel regulator of stress and heat shock response, controls *clp* and molecular chaperone gene expression in gram-positive bacteria. Mol. Microbiol. 31:117–131.
7. Diamant, S., D. Rosenthal, A. Azem, N. Eliahu, A. P. Ben-zi, and P. Goloubinoff. 2003. Dicarboxylic amino acids and glycine-betaine regulate chaperone-mediated protein-disaggregation under stress. Mol. Microbiol. 49:401–410.
8. Ekaza, E., J. Teyssier, S. Ouahrani-Bettache, J. P. Liautard, and S. Köhler. 2001. Characterization of *Brucella suis clpB* and *clpAB* mutants and participation of the genes in stress responses. J. Bacteriol. 183:2677–2681.
9. Eriksson, M. J., and A. K. Clarke. 1996. The heat shock protein ClpB mediates the development of thermotolerance in the cyanobacterium *Synechococcus sp.* strain PCC 7942. J. Bacteriol. 178:4839–4846.
10. Fukuda, D., M. Watanabe, S. Sonezaki, S. Sugimoto, K. Sonomoto, and A. Ishizaki. 2002. Molecular characterization and regulatory analysis of *dnaK* operon of halophilic lactic acid bacterium *Tetragenococcus halophila*. J. Biosci. Bioeng. 93:388–394.
11. Glover, J. R., and S. Lindquist. 1998. Hsp104, Hsp70, and Hsp40: a novel chaperone system that rescues previously aggregated proteins. Cell 94:73–82.
12. Goloubinoff, P., A. Mogk, A. P. B. Zvi, T. Tomoyasu, and B. Bukau. 1999. Sequential mechanism of solubilization and refolding of stable protein aggregates by a bichaperone network. Proc. Natl. Acad. Sci. USA 96:13732–13737.
13. Ingmer, H., F. K. Vogensen, K. Hammer, and M. Kilstrup. 1999. Disruption and analysis of the *clpB*, *clpC*, and *clpE* genes in *Lactococcus lactis*: ClpE, a new Clp family in gram-positive bacteria. J. Bacteriol. 181:2075–2083.
14. Kim, K. I., G. W. Cheong, S. C. Park, J. S. Ha, K. M. Woo, S. J. Choi, and C. H. Chung. 2000. Heptameric ring structure of the heat-shock protein ClpB, a protein-activated ATPase in *Escherichia coli*. J. Mol. Biol. 303:655–666.
15. Krzewska, J., G. Konopa, and K. Liberek. 2001. Importance of two ATP-binding sites for oligomerization, ATPase activity and chaperone function of mitochondrial Hsp78 protein. J. Mol. Biol. 314:901–910.
16. Lee, G. J. 1995. Assaying proteins for molecular chaperone activity. Methods Cell Biol. 50:325–334.
17. Lee, S., M. E. Sowa, Y. Watanabe, P. B. Sigler, W. Chiu, M. Yoshida, and F. T. F. Tsai. 2003. The structure of ClpB: a molecular chaperone that rescues proteins from an aggregated state. Cell 115:229–240.
18. Lindquist, S., and G. Kim. 1996. Heat-shock protein 104 expression is sufficient for thermotolerance in yeast. Proc. Natl. Acad. Sci. USA 93:5301–5306.
19. Mogk, A., T. Tomoyasu, P. Goloubinoff, S. Rüdiger, D. Röder, H. Langen, and B. Bukau. 1999. Identification of thermolabile *Escherichia coli* proteins: prevention and reversion of aggregation by DnaK and ClpB. EMBO J. 18:6934–6949.
20. Motohashi, K., Y. Watanabe, M. Yohda, and M. Yoshida. 1999. Heat-inactivated proteins are rescued by the DnaK · J-GrpE set and ClpB chaperones. Proc. Natl. Acad. Sci. USA 96:7184–7189.
21. Namy, O., M. Mock, and A. Fouet. 1999. Co-existence of *clpB* and *clpC* in the Bacillaceae. FEMS Microbiol. Lett. 173:297–302.
22. Parsell, D. A., A. S. Kowal, and S. Lindquist. 1994. *Saccharomyces cerevisiae* Hsp104 protein. Purification and characterization of ATP-induced structural changes. J. Biol. Chem. 269:4480–4487.
23. Robert, H., C. L. Marrec, C. Branco, and M. Jebbar. 2000. Glycine betaine, carnitine, and choline enhance salinity tolerance and prevent the accumulation of sodium to a level inhibiting growth of *Tetragenococcus halophila*. Appl. Environ. Microbiol. 66:509–517.
24. Sanchez, Y., and S. Lindquist. 1990. HSP104 required for induced thermotolerance. Science 248:1112–1115.
25. Schirmer, E. C., C. Queitsch, A. S. Kowall, D. A. Parsell, and S. Lindquist. 1998. The ATPase activity of Hsp104, effects of environmental conditions and mutations. J. Biol. Chem. 273:15546–15552.